TEMPERATURE MEASUREMENTS OF LARGE POWER ARCS AND THE RELATION OF TEMPERATURE TO DIELECTRIC RECOVERY

Thesis by

William Charles Duesterhoeft, Jr.

In Partial Fulfillment of the Requirements

For the Degree of

Doctor of Philosophy

California Institute of Technology

Pasadena, California

1953

ACKNOWLEDGMENT

The author wishes to express his sincere appreciation for the interest and guidance given by Professor G. D. McCann. He acknowledges the many helpful suggestions and generous cooperation of Dr. R. B. King during the spectrographic study. The author is greatly indebted to Mr. J. E. Conner for his valuable assistance in obtaining the data and for his many helpful suggestions throughout the course of the research. He also acknowledges the valuable assistance rendered by Mr. R. B. Shennum and Mr. W. C. Pilkington in obtaining the data.

The work was supported by the Kelman Electric and Manufacturing Co., the Southern California Edison Co., and the Department of Water and Power of the City of Los Angeles. The research was made possible through their interest in dielectric recovery research. The author wishes to express his appreciation for their assistance.

The author is indebted to Mrs. Edith Lilley for typing the thesis.

SUMMARY

A study of the basic mechanism of dielectric recovery of power frequency arcs in air is reported. The particular arc studied is that of a standard 6 inch rod gap conducting 300 or 800 amperes crest for 1/2 cycle of a 60 cycle per second current.

The temperature of the arc space and the variation of the arc temperature with time are measured. The temperature is measured by spectrographic and velocity of sound techniques. The temperature at current zero is 5000 degrees Kelvin. The temperature is 720 degrees K. 77 milliseconds after current zero and 415 degrees K. 196 milliseconds after current zero.

The temperature is correlated to the dielectric strength during the recovery period. During the recovery period the arc space is at atmospheric pressure. The gas density is reduced due to the high temperatures existing in the arc space. Evidence is given that the low gas density is the major factor causing the reduced dielectric strength.

Residual ions in the arc space also contribute to reducing the dielectric strength. A criterion for recovery breakdown is given including the effect of the residual ions. The ion density after current zero decreases due to electron recombination with a recombination coefficient $\alpha = 2.0 \times 10^{-9}$ cubic centimeter per ion-second. The loss of ions by diffusion appears negligible.

Introduction

The rates at which large air gaps recover dielectric strength after the conduction of power frequency currents are of prime importance to the electrical transmission engineer. A fundamental understanding of the various factors affecting the recovery mechanism is also important.

The dielectric recovery period can be separated into regions of two distinctly different phenomena. Immediately after current zero the strength of the arc space is affected by both the density of the gas and the density of the residual ions in the arc space. Later, after sufficient decrease of ion density, the dielectric strength of the gas is determined primarily by the gas density. The term dielectric strength as applied here to the gas with appreciable ion density when the gas is a conductor is taken to mean that critical value of applied voltage above which the conductance of the gas increases until a stable conducting state is reached or below which the conductance decreases until a stable insulating state is reached. Since the gas density can be determined from the temperature, knowledge of the variation of the temperature with time in the arc space is important in segregating the recovery period into the above mentioned regions.

Temperature measurements of the hot gases of the arc space of 1/2 cycle, 300 and 800 ampere crest, 6 inch arc discharges between steel electrodes are described in this thesis. The results for the 800 ampere, 1/2 cycle discharge

may be summarized briefly as follows. The temperature at current zero is 5000° K. and the rate of decrease at current zero is approximately 10^5 degrees K. per second. The temperature is 720° K. 77 milliseconds after current zero and 415° K. 196 milliseconds after current zero. After some 60 milliseconds of recovery time the dielectric strength can be accounted for solely by the gas density. Throughout the recovery period the low gas density is a major factor contributing to the low dielectric strength. Residual ions effect a reduction in the dielectric strength for recovery times shorter than 60 milliseconds. A criterion for recovery strength is applied to the period during which the ion density is appreciable in order to compute the ion density during this period. The variation of the ion density indicates that the loss of ions is due to recombination with a recombination coefficient of $\alpha = 2.0 \times 10^{-9}$ cubic centimeter per ion-second. The loss of ions by diffusion from the open gap appears negligible.

Dielectric recovery rates of large air gaps are important to electrical transmission engineers in determining the minimum reclosing times of reclosing circuit breakers. When faults occur on transmission systems, the tie between generating center and load center is weakened; the transfer reactance is increased, and thus less power is transferred. Since governors are inherently relatively slow, the machines at the generating center accelerate while those near the load center decelerate; and the system begins to lose synchronism. Minimizing the effect of the

fault on the stability of the system requires both quick isolation of the faulted section and quick reinsertion of the faulted section after the fault has recovered. The amount of power that can be transmitted reliably - that is, with assurance that the system remains in synchronism after a fault occurs - is dependent on both the speed of the relay and circuit breaker operation and the circuit breaker reclosure time. With recent developments in high-speed reclosing circuit breakers, the dielectric recovery of the faulted arc space is important in determining the minimum permissible reclosure time.

Most dielectric recovery data taken in the past are from short arcs for which electrode effects play a predominant role.* Such data are applicable to determining the reignition or extinction characteristics of alternating current arcs as those at circuit breaker contacts. Data on the recovery characteristics of large power arcs in long gaps are rather meager. Some data have been obtained indirectly from staged tests on actual systems where minimum time of reclosure was obtained by test (3, 4).* Since the availability of power systems for such staged tests is definitely limited, laboratory methods have been developed. Boisseau, Wyman, and Skeats obtained direct

---

* For excellent discussions of the definitions of and the difference in the extinction of the short and long arc, see references 1 and 2. For all numbered references see the bibliography at the end of this thesis.

reclosure data from tests on system models (5). Although these tests gave excellent results regarding the probability of successful reclosure, basic information on the variation of recovery with the many important factors involved could not be obtained because many of these factors could not be controlled. McCann, Conner, and Ellis developed a test technique whereby recovery characteristics could be determined in the laboratory (6). This technique allowed control of most of these influencing factors. Much direct recovery information could be obtained with relative ease. McCann, Conner, and Ellis obtained rather extensive data on arcs up to 300 amperes in air gaps up to 11 inches long. Ellis has presented more data obtained by the same technique (7). Although these data are empirical in nature, they are directly applicable to a fundamental study of the recovery process since so many factors were controlled. Since it is recognized that a basic understanding of the recovery mechanism should be important to the engineer, the fundamental study of this thesis was undertaken. The research complements the work of McCann, Conner, and Ellis which was performed in the California Institute of Technology High Potential Laboratory.

Knowledge of the decay of the temperature of the gases in the arc space after current extinction is basic in such a fundamental study. Knowledge of the temperature should help explain the importance of the effects of

(1) The degree of ionization in the arc

space and its variation including the relative effects of diffusion and recombination.

(2) The variation of the ionizing coefficients for the second breakdown including the effect of the reduced density of the hot gases in the arc space.

The purpose of the research reported in this paper was to determine the variation of the temperature in the arc space and to correlate this temperature to dielectric recovery. The particular arc space studied was that of a standard 6 inch rod gap during and after conduction for 1/2 cycle of 300 and 800 ampere crest, 60 cps, current.

The temperatures of electric arcs have been determined by spectrographic techniques (8, 9) and by velocity of sound measurements (10). Both of these techniques were employed for the research of this paper. Time resolved temperatures of damped electric sparks have previously been determined by the spectrographic technique (11).

Spectrographic Determination of Temperature

Apparatus and Test Technique. The research was performed on an arc in a standard rod gap, 6 inches long with 1/2 inch square steel electrodes. The apparatus and method of obtaining gap breakdown with subsequent controlled 1/2 cycle power follow current has been described in previous reports (6, 7). A schematic block diagram of this experiment is shown as Fig. 1. Before a test shot, 2500 volt, 60 cps potential was applied to the gap G. The surge generator was tripped from the phase controlled pulse circuit at the proper phase to cause sinusoidal power current to follow the surge generator breakdown of the test gap and stand-off gap G. The current was cut-off after 1/2 cycle by bias applied to ignitrons in the power circuit. The ignitron bias control circuit operation was initiated by a pulse picked up through C_1, a porcelain insulator. The magnitude of the arc current was controlled by the reactor X. The low pass filter shown at the gap G protected the power equipment from the surge pulse. For detailed description of this circuit including schematic diagrams of the circuits shown as boxes in Fig. 1 see references 6 or 7.

The spectrograph was exposed to the luminous gases of the arc space for a time corresponding to 20 electrical degrees, 926 microseconds, through a slot cut in a disc D. The disc D was rotated by a 4-pole synchronous motor M. The synchronous motor was supplied voltage from a phase shifter;

and the particular time, over a 2 cycle period, during which the spectrograph was exposed was determined by the phase shifter setting.

The phase controlled trip pulse was obtained from a peaking transformer supplied by a selsyn phase shifter. The peaking transformer output was sharpened by additional circuitry. This pulse was applied to the plate of a 2D21 thyratron. A cam operated switch on the motor shaft supplied a square wave bias to the control grid of the 2D21. The surge generator was tripped when this plate pulse appeared with zero bias and was not tripped when the bias was negative. This allowed the surge generator to be tripped only when the disc slot was over a particular pair of poles. See Fig. 2. Whether or not the motor had synchronized on the correct pole could be determined from a lissajous figure on an oscilloscope with 60 cps voltage and the cam switch output connected to its plates. Magnetic oscillographs were taken of all shots of arc current and the cam switch output to assure that the spectrograph was exposed at the desired instant.

The arc was focused on the spectrograph slit by a 2 1/2 inch diameter glass lens such that the image size at the slit was 1/3 the object size. The spectrograph was a Hilger instrument with a Littrow type mounting. The dispersion of the blue lines used was 150 A^{o} per inch. The spectrum observed was the line spectrum of the neutral iron atom.

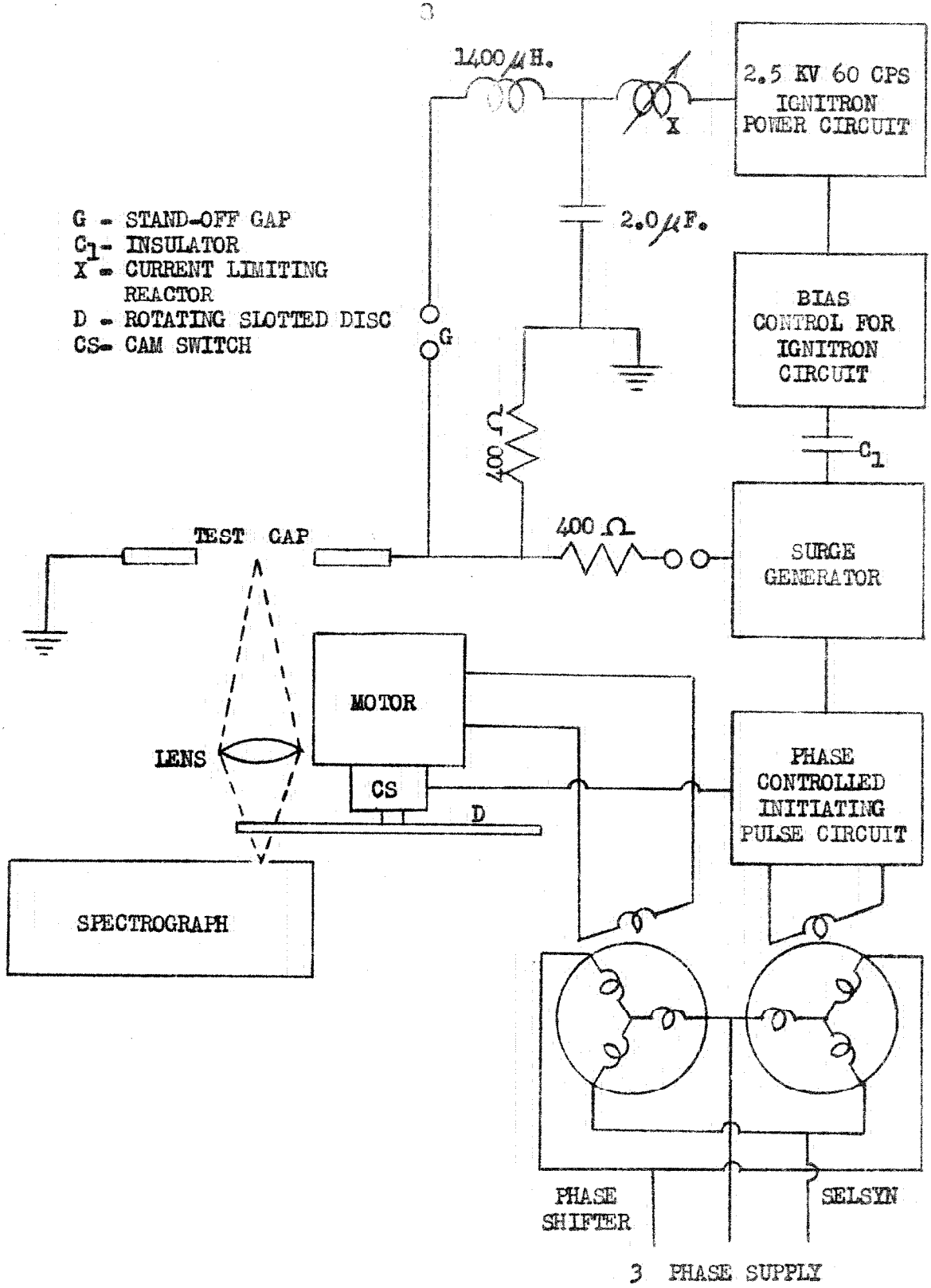

FIG. 1 SCHEMATIC BLOCK DIAGRAM OF SPECTROGRAPHIC EXPERIMENTS

Since it was important that the relative intensities of the various iron lines be measured accurately, much time was spent developing the photographic photometry technique. Each photographic plate was calibrated in per cent transmission as determined by a recording microdensitometer versus relative intensity. The densitometer was used to plot the calibration and to scale the lines. The exposure for calibration of the spectrograph plate was obtained by placing a calibrated step weakener (a coated glass plate of known steps of per cent transmission) at the slit and illuminating the slit uniformly.

Since each plate was calibrated, errors which may arise from the differences in the development of different plates were eliminated. The step weakener used was made from very fine grain Kodak 649 plate with steps of varying degrees of exposure. This weakener of silver on glass is not achromatic but was considered so over the small portion of spectrum used; namely, 4202 A^{o} to 4529 A^{o}. The step weakener was calibrated by means of the inverse square law. An exposure through the step weakener was compared with exposures at varying distances from a point Hg source. The Hg 4358 A^{o} line was used for this calibration.

Each spectrographic plate was calibrated by a flash of light of the same time duration as the arc exposures. Thus, errors due to the emulsion reciprocity law failure were eliminated. The arc and rotating disc with its slot were used for this calibrating exposure. Uniform exposure of the

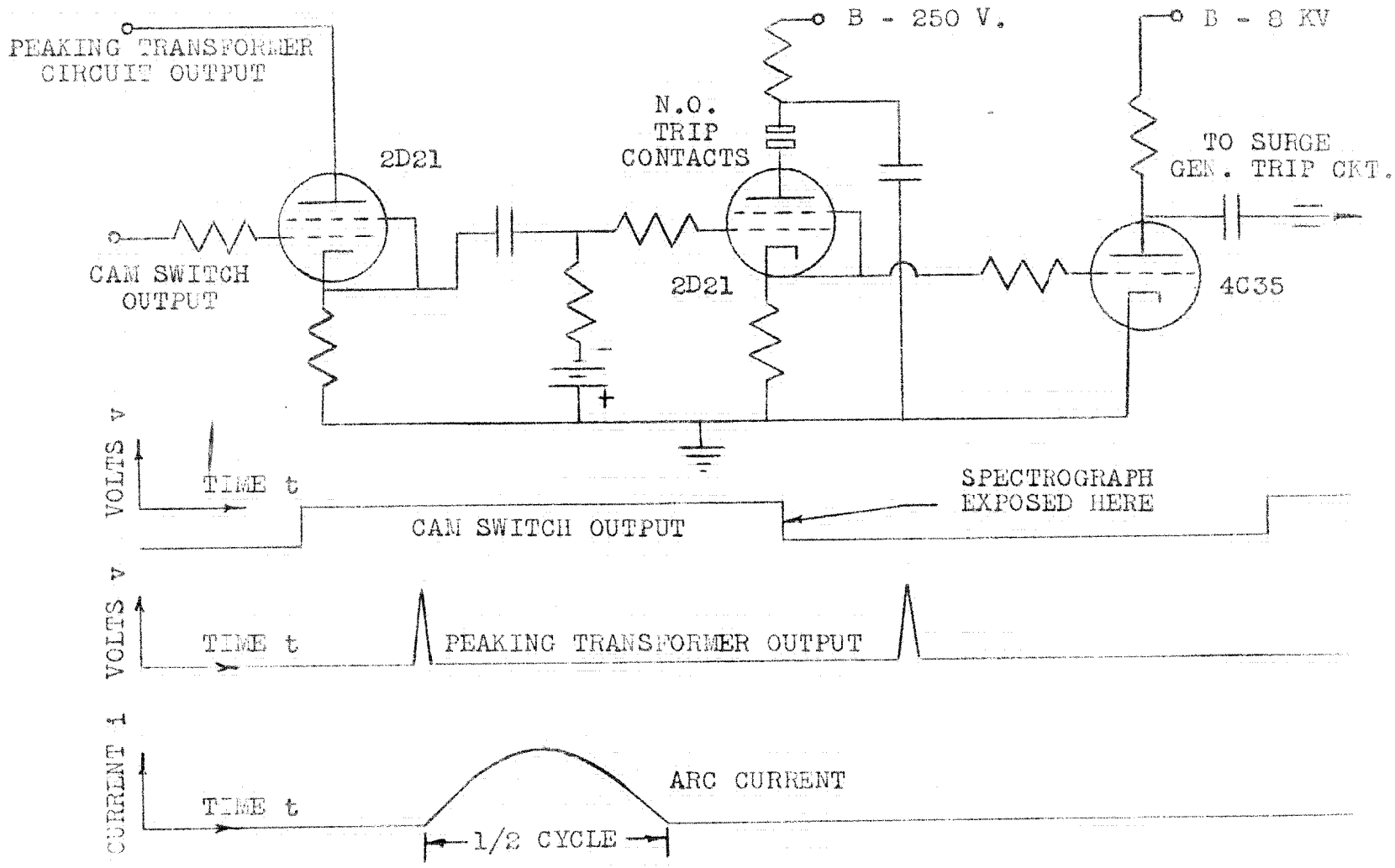

FIG. 2 2D21 TRIP CIRCUIT AND CURVES OF PEAKING TRANSFORMER CIRCUIT OUTPUT, CAM SWITCH OUTPUT, AND 1/2 CYCLE OF ARC CURRENT. THE RELATIVE PHASE OF THE CAM SWITCH OUTPUT IS CONTROLLED BY THE PHASE SHIFTER SETTING.

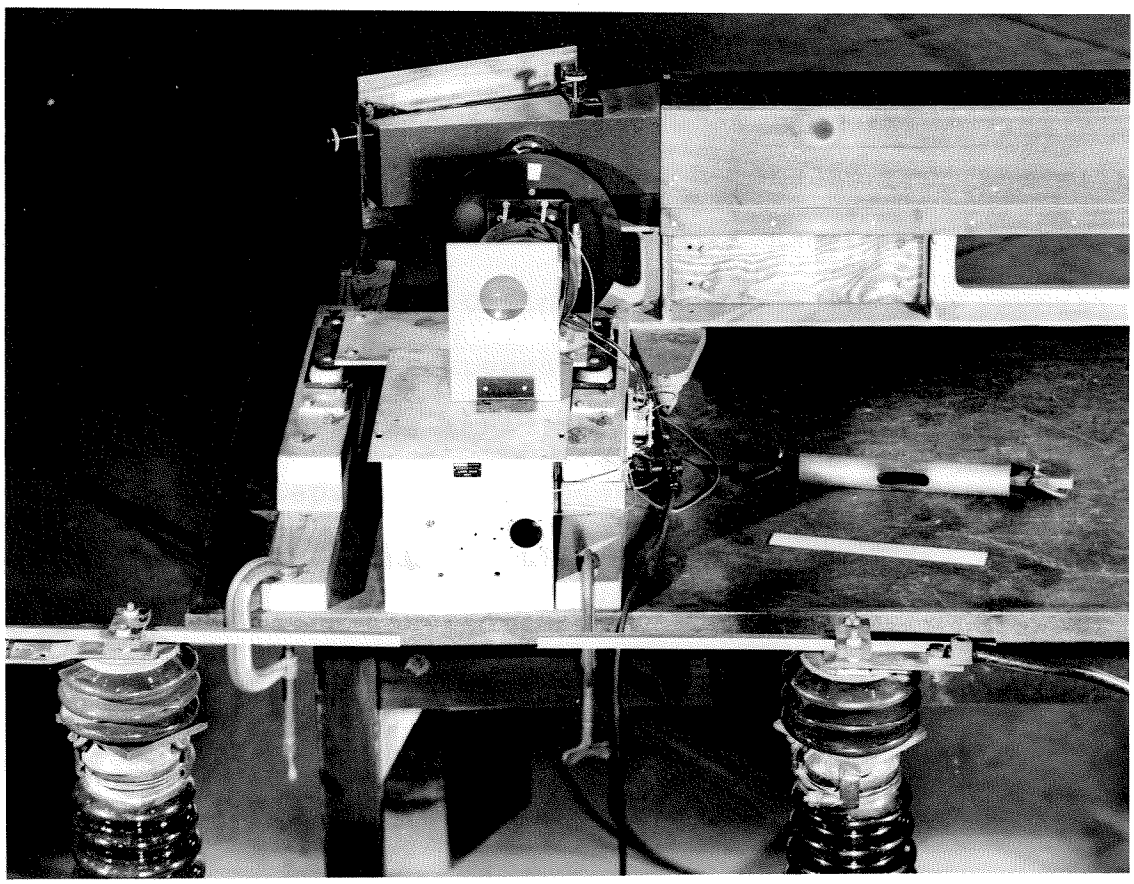

FIG. 3 PHOTOGRAPH OF EQUIPMENT USED FOR SPECTROGRAPHIC TECHNIQUE SHOWING TEST GAP, LENS, MOTOR AND DISC, AND SPECTROGRAPH. THE TUBE FOR CALIBRATION EXPOSURES IS SHOWN ON THE TABLE.

spectrograph slit was obtained by removing the lens while the arc was confined to the inside of a 3/4 inch I.D., 1 3/4 inch O.D. fiber tube with a 3/4 inch by 3 inch window. The light from this window was used for the calibration. Since this window was 64 inches from the slit, quite uniform illumination of the slit was obtained. It was found that the loss of intensity caused by the removal of the lens could be compensated for by inserting a small #36 copper wire in the tube for enhanced emission during calibration. Separate electrodes were used during calibration to prevent contamination of the test electrodes with copper. The micro-densitometer calibration tracings were taken along some line near the center of the spectrum used. In order to facilitate tracing along this line, a slit opening as large as 0.60 mm. was used for calibration exposures.

For the test spectrograms, the slit openings used were as large as allowed by the dispersion of the spectrograph without causing objectionable blending of lines; namely, 0.12 to 0.18 mm. Thus a microdensitometer slit which was large compared to the emulsion grain size could be used; consequently, variations of the tracings due to grain size were minimized. With this slit opening the central intensity could be used as the intensity of the line.

Kodak 50 and Kodak Panatomic X plates were used. The Panatomic X plates were more desirable; however, the supply was limited. Most of the data were taken from Kodak 50

plates. During development, the developer tray was agitated by rocking to give even development and reduce the Eberhardt effect.

Spectrograms taken during the time of actual power current flow gave sufficient exposure in a single shot; however, the light intensity of the iron spectrum in the after-glow decreased so rapidly after current zero that for sufficient exposure of the plates multiple shots had to be superimposed. Suitable exposures were obtained with 10 shots 10 degrees after current zero and with 30 shots 180 degrees after current zero. Calibrations were made with the same number of shots as used for test exposures.

Theory of Temperature Determination. If the atoms of a gas are thermally excited so that some of the electronic energy states other than the ground state are populated, the gas emits a line spectrum. Each line is the result of transitions of the atoms from one particular state or energy level to another particular energy level of lower energy. In thermal excitation the excitation is due to collisions of the gas particles. The intensity of a line relative to the intensity of another line depends upon the temperature of the source. At low temperature there will be very few atoms in excited states. With an increase in temperature the number in the higher states will increase, and hence, the rate of transitions from the higher states will increase. If the "oscillator strengths" (sometimes called "f-values" or "transition probabilities") are known and the relative intensities of the lines can be measured, the relative population densities of the various energy levels can be computed. Conversely, if the population densities are known, the intensities can be predicted. In the high pressure electrical arc discharge atoms are excited not only by collisions with other atoms but with electrons; however, Ornstein, Mannkopf, and others have shown that in the high pressure arc the electron temperature and gas temperature are essentially the same (8, 9).

The iron spectrum is very rich in lines. The "f-values" of many of the iron lines have been measured (12, 13).

The method used here is to assume that the population

densities are given approximately by the Maxwell-Boltzman distribution with the temperature unknown. Then

$$(1) \qquad N_m/g_m = (N_n/g_n)\epsilon^{-(E_m - E_n)/kT}$$

where N_i is the number of atoms in level i whose statistical weight is g_i and whose excitation potential is E_i. T is the temperature. k is Boltzman's constant.

The oscillator strength f_{nm} is defined by

$$(2) \qquad I = (N_m/g_m)\, g_n f_{nm}\, \nu^3 K$$

where I is the intensity of frequency ν and K is a constant given by

$$K = \frac{8\pi^2 e^2 h}{m c^3}$$

If Eq. 2 is substituted in Eq. 1, there results

$$(3) \qquad \log_{10} (I/g_n f_{nm} \nu^3) = \text{const.} - 5040E_m/T$$

where I is the relative intensity of the line whose upper level is E_m in volts. If points for a number of lines are plotted

$$\log_{10} (I/g_n f_{nm} \nu^3) \quad \text{versus} \quad E_m$$

the result should be a straight line with a slope $m = -5040/T$.

The lines which were used are listed in Table 1. The

f-values are those of R. B. King and A. S. King and of W. W. Carter (12, 13). The values for E_m were obtained from Henry N. Russell and Charlotte E. Moore (15).

Table 1

List of Iron Lines Used in Temperature Determination

λ	gf	$\log_{10}(\lambda^3/gf)$	E_m
4202.0	890	7.92	4.44
4206.7	0.60	11.09	2.99
4216.2	2.14	10.54	2.94
4219.4	25800	6.46	6.50
4222.2	1320	7.76	5.38
4227.4	22300	6.53	6.25
4231.5	11000	6.84	6.17
4233.6	2790	7.43	5.40
4235.9	4620	7.22	5.35
4238.8	11100	6.84	6.30
4247.4	9880	6.89	6.28
4260.5	8130	6.98	5.30
4282.4	2280	7.54	5.06
4294.1	380	8.32	4.37
4299.2	2120	7.57	5.30
4307.9	3300	7.38	4.43
4325.8	3800	7.33	4.46
4375.9	4.4	10.28	2.83
4383.6	5800	7.16	4.31
4404.8	3000	7.45	4.37
4415.1	1000	7.94	4.41
4427.3	4.3	10.30	2.85
4447.7	709	8.09	5.00
4454.4	2470	7.55	5.60
4459.1	1070	7.92	4.95
4476.0	2500	7.56	5.60
4494.6	1240	7.86	4.95
4528.7	2100	7.98	4.90

Results. A typical spectrogram is shown as Fig. 4. Fig. 5 shows a typical microdensitometer tracing; the calibration tracing is included. The calibration curve of Fig. 6 shows percent densitometer reading versus relative intensity. Two examples of the temperature determination curves are shown as Fig. 7 and Fig. 8. θ is the time in electrical degrees measured from the start of the power current. The results of the spectrographic measurements are shown in Figs. 9a and 9b. Little change in temperature was expected as the spectrograph was focused at different points along the arc. This was observed. It was observed that after current zero the intensity decreased more rapidly from regions near the electrodes than from the gap center. The electrodes tend to cool the gas surrounding them.

With the spectrograph focused in the center of the gap, the iron spectrum was not observed until after approximately 55 electrical degrees of current conduction. Images of the iron lines could be observed much earlier in the half-cycle of current conduction with the spectrograph focused near either electrode. With the spectrograph focused 5 inches from the ground electrode, the spectrum was observed after 25 electrical degrees. This time lag was probably due to the finite time required for the iron vapor to evaporate and travel to the center of the gap with a velocity of approximately 3.6×10^3 cm. per second. Many of the spectrograms taken during the first quarter cycle of current conduction exhibited a pronounced continuous background. Fig. 10 shows

a spectrogram with this continuum. This continuum could be due to pressure broadening and blending of the many iron lines, for the pressures must be very great during the first few milliseconds of conduction. The explosive nature of the discharge could result in discrete particles of iron being blown out of the electrodes with a resulting black body type of emission from these particles. The continuum is most probably due to the pressure broadening for the background does appear as very broad 'lines' or bands.

The size of the luminous region as observed on the spectrograms agrees with observations made with 3000 frame per second motion pictures reported by McCann, Conner, and Ellis and by Ellis. Early in the period of conduction the diameter of the core is small compared to its dimensions after several milliseconds of conduction. Core sizes are known to be a function of the pressure. After the arc develops, it expands radially reaching diameters of several inches. The photographs of Ellis show little change in shape of the luminous region after current zero except that due to the cooling of the hot gas.

Due to the rapid decrease in the intensity of the iron lines with time, plate exposures were difficult to obtain at appreciable times after current zero; i.e. 8 milliseconds or 1/2 cycle after current zero. A velocity of sound technique was used to determine the temperature at these times. This technique and the results obtained are discussed in the next sections.

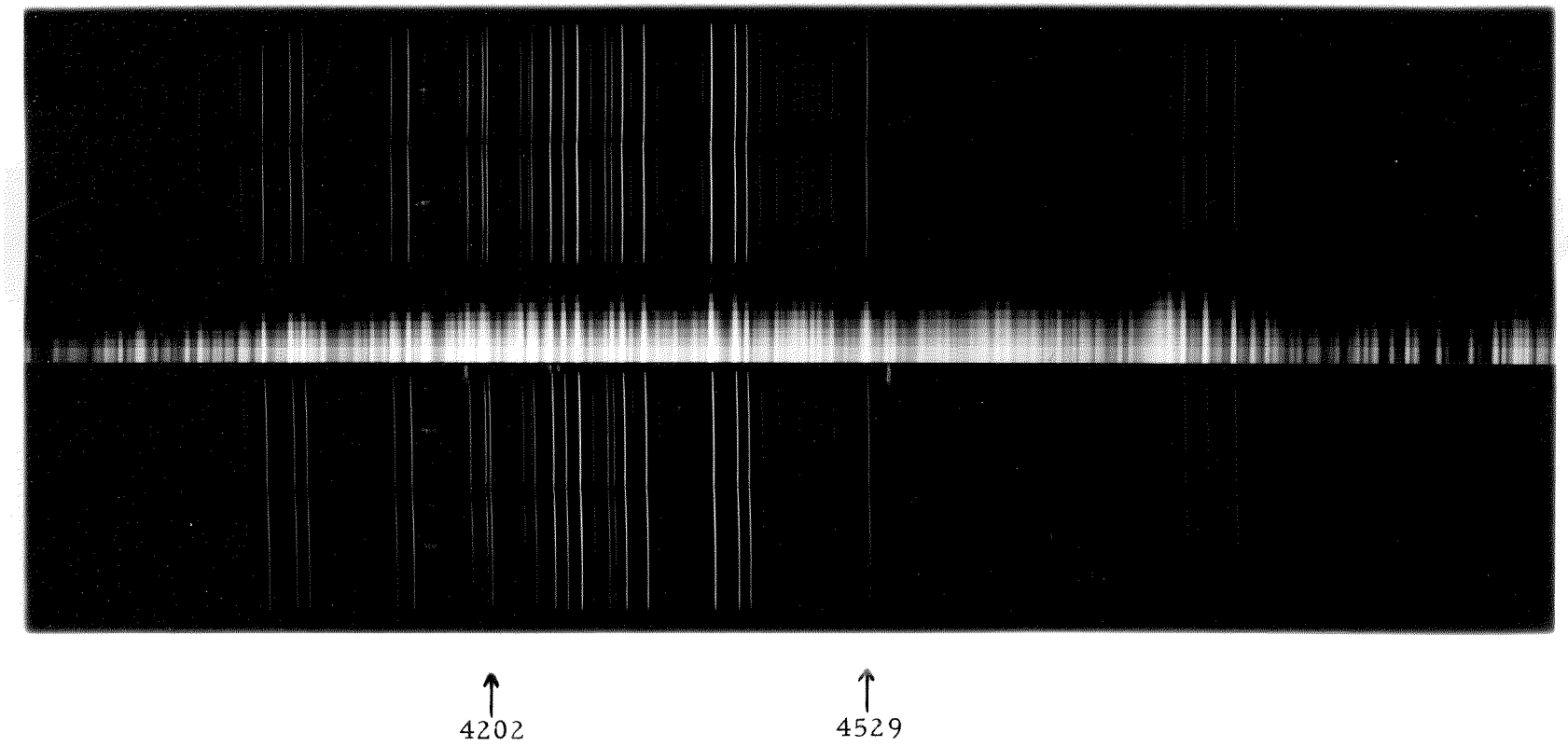

Fig. 4 SPECTROGRAPH PLATE NO. 106 SHOWING CALIBRATION EXPOSURE AND 4 TEST EXPOSURES OF 20 SHOTS EACH.

800 amperes 1/2 cycle θ=270 elec. degrees Focus center of gap

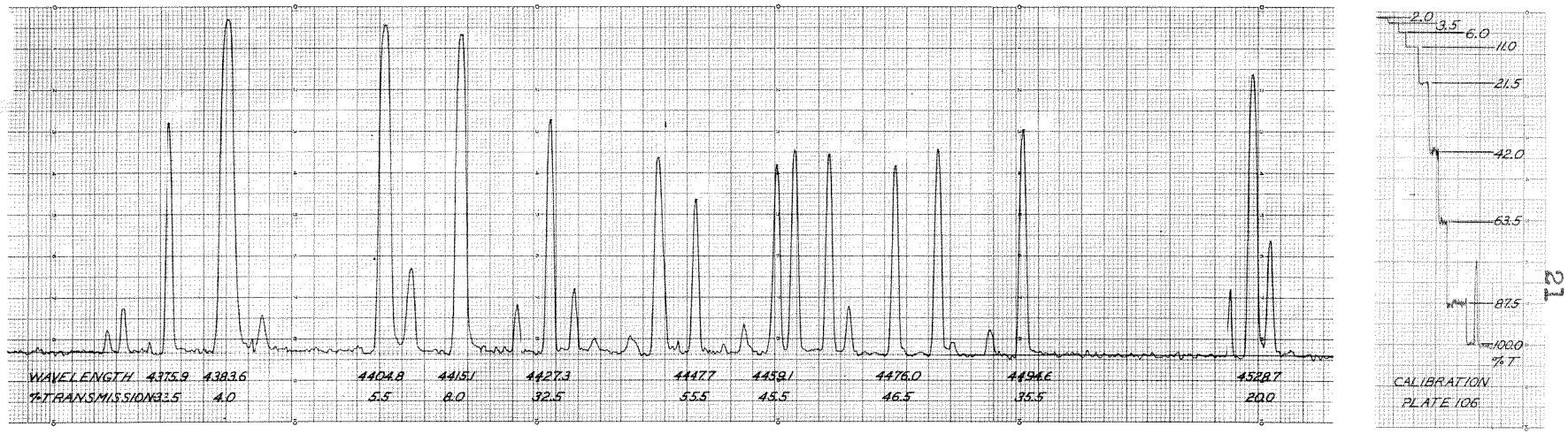

Fig. 5 TYPICAL MICRODENSITOMETER TRACING WITH CALIBRATION AT RIGHT.

PLATE 106B
6 INCH GAP 800 AMPERES - 1/2 CYCLE
FOCUS CENTER OF GAP θ=270 ELEC. DEGREES

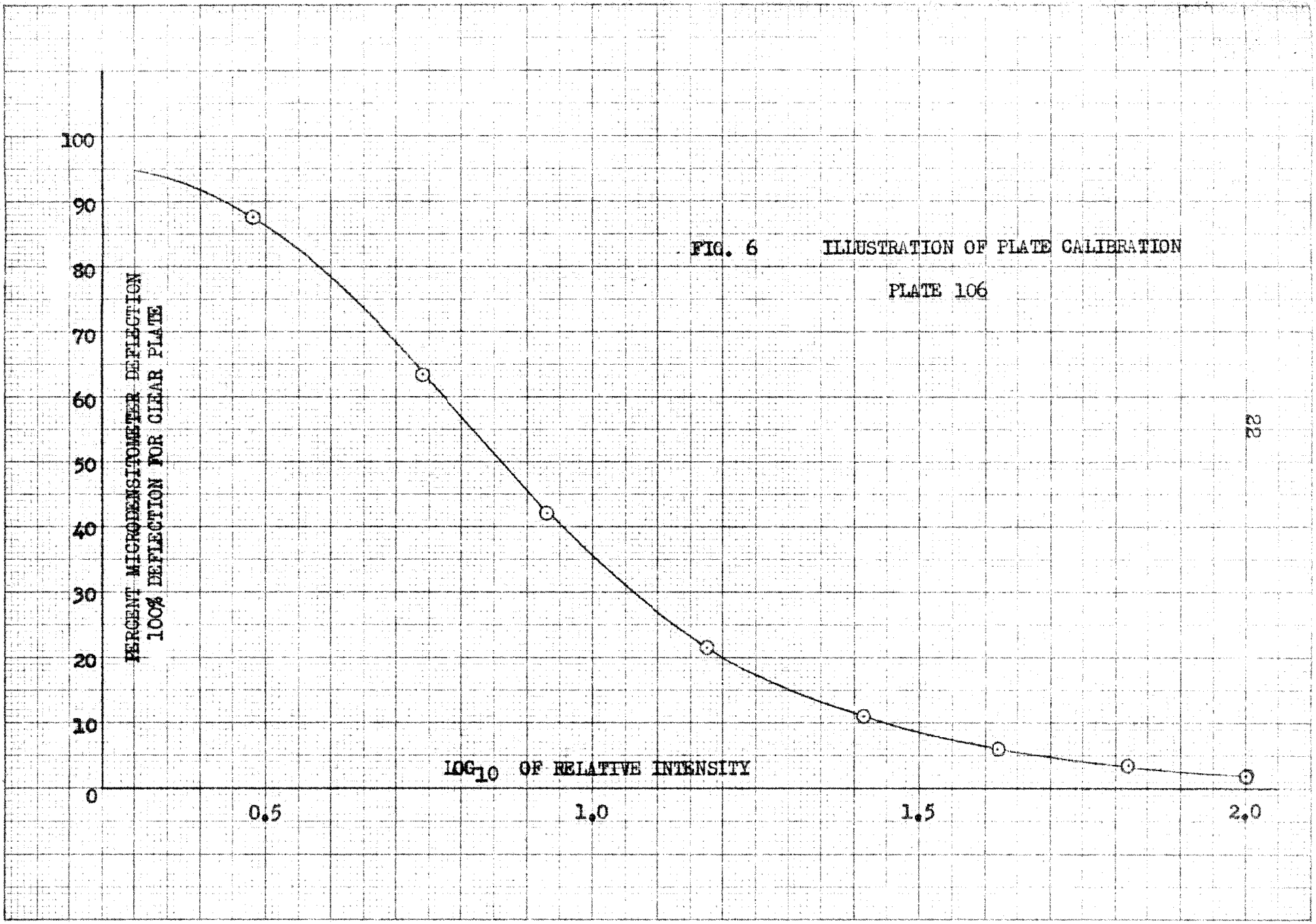

FIG. 6 ILLUSTRATION OF PLATE CALIBRATION

PLATE 106

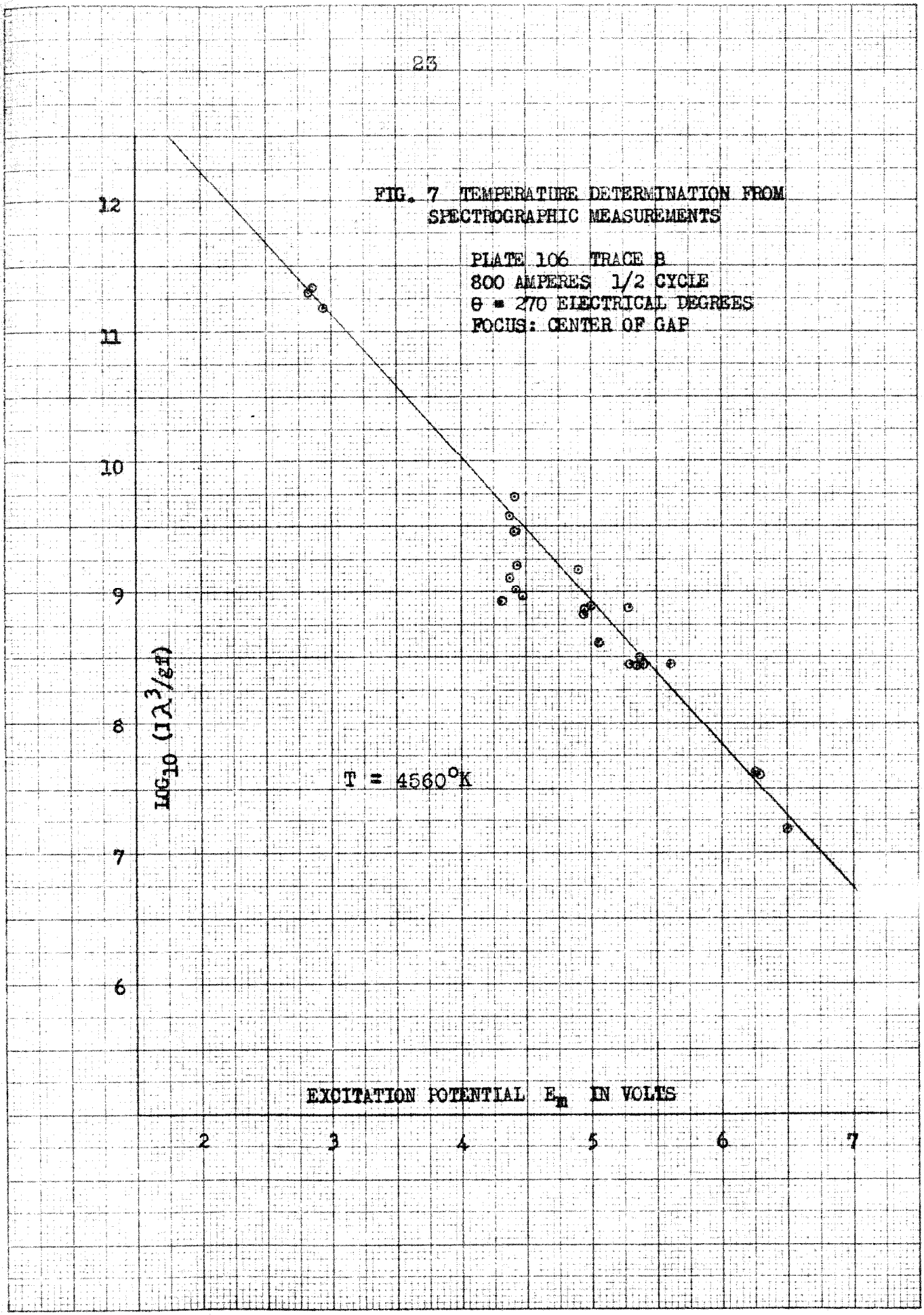

FIG. 7 TEMPERATURE DETERMINATION FROM SPECTROGRAPHIC MEASUREMENTS

PLATE 106 TRACE B
800 AMPERES 1/2 CYCLE
θ = 270 ELECTRICAL DEGREES
FOCUS: CENTER OF GAP

FIG. 8 TEMPERATURE DETERMINATION FROM SPECTROGRAPHIC MEASUREMENTS

PLATE 85 TRACE B
800 AMPERES 1/2 CYCLE
θ = 135 ELECTRICAL DEGREES
FOCUS 5 INCHES FROM GROUND ELECTRODE

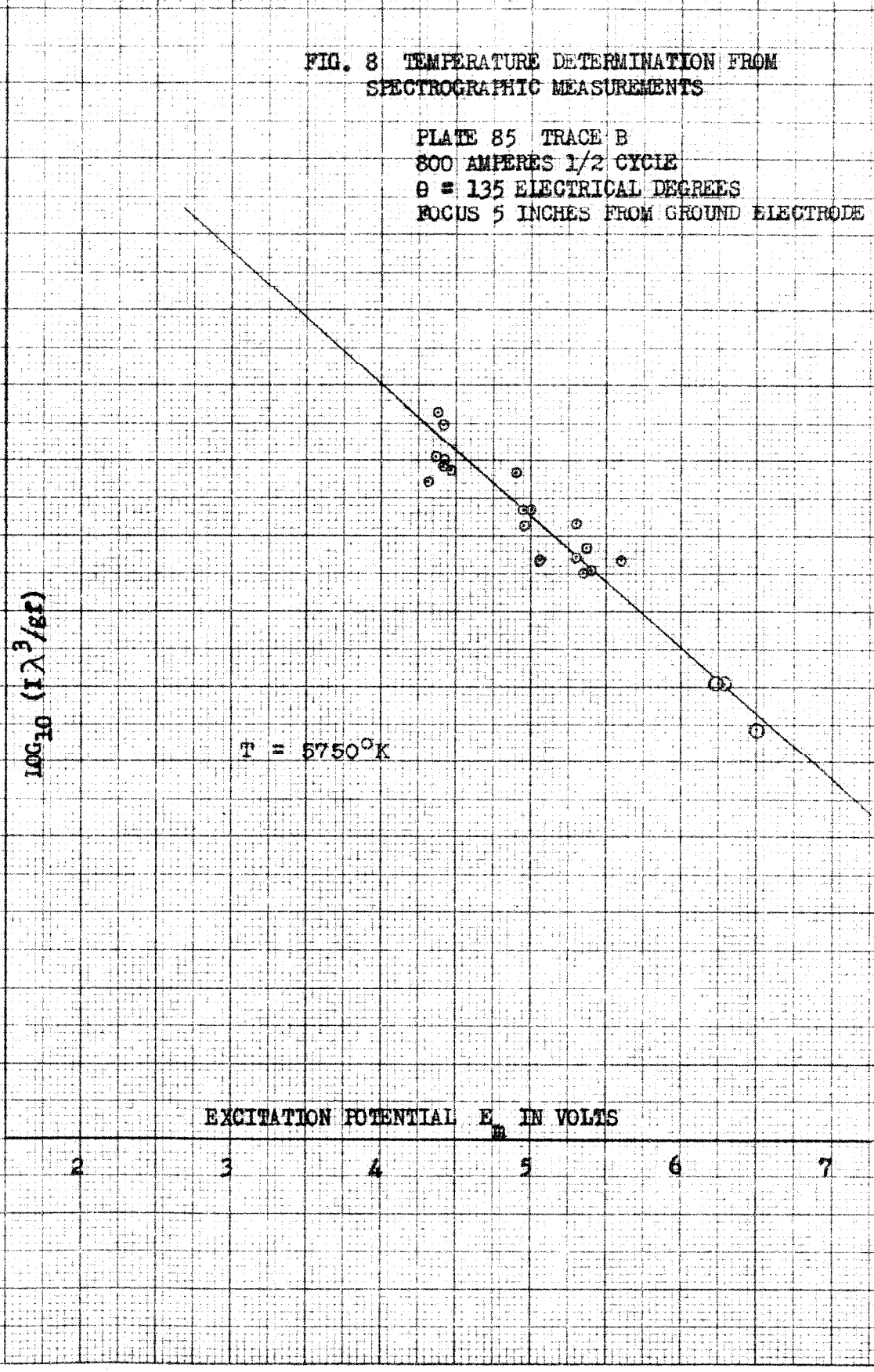

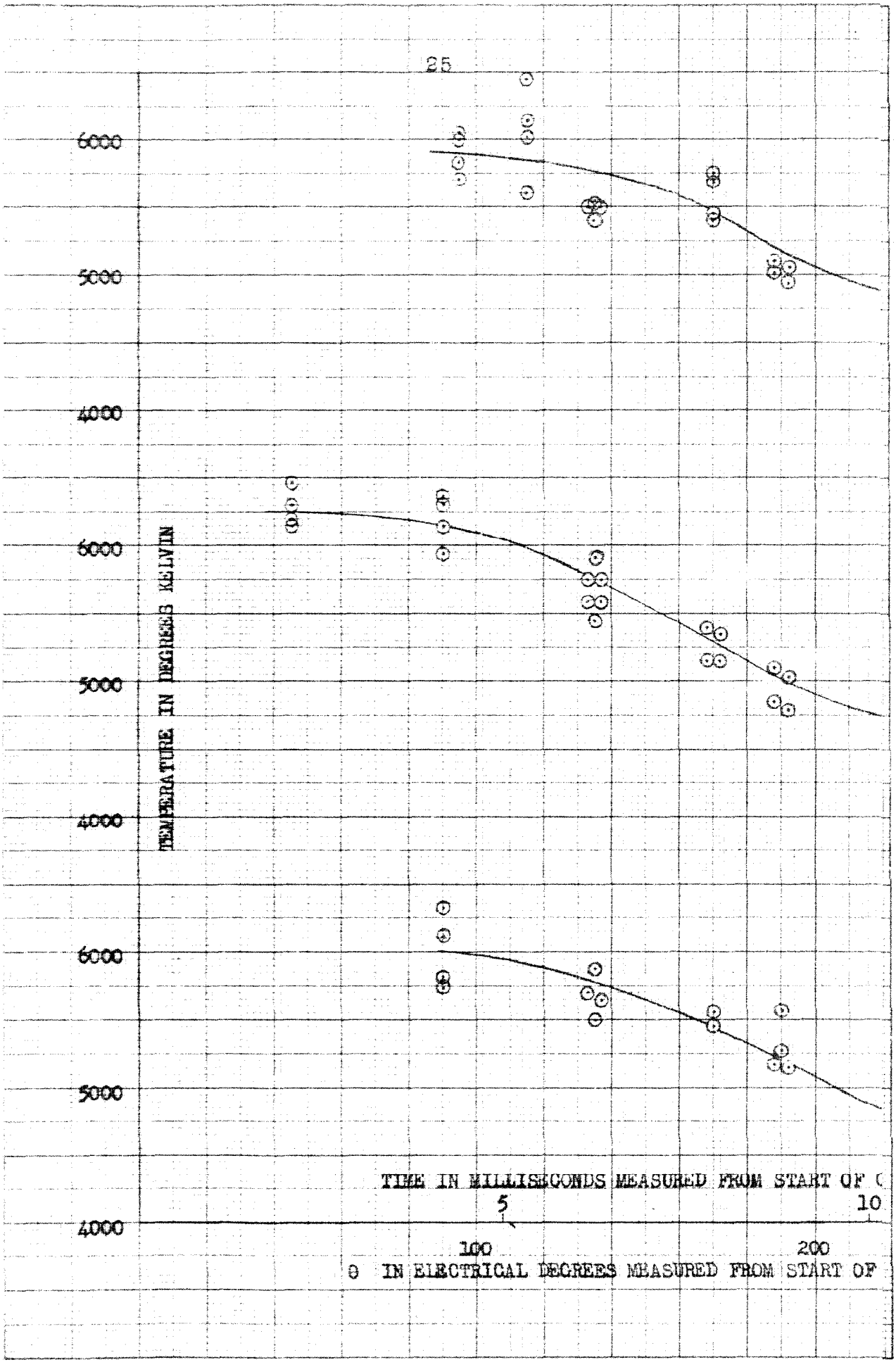
25
6000
5000
4000
6000
5000
4000
6000
5000
4000
TEMPERATURE IN DEGREES KELVIN
TIME IN MILLISECONDS MEASURED FROM START OF
5
10
100
200
θ IN ELECTRICAL DEGREES MEASURED FROM START OF

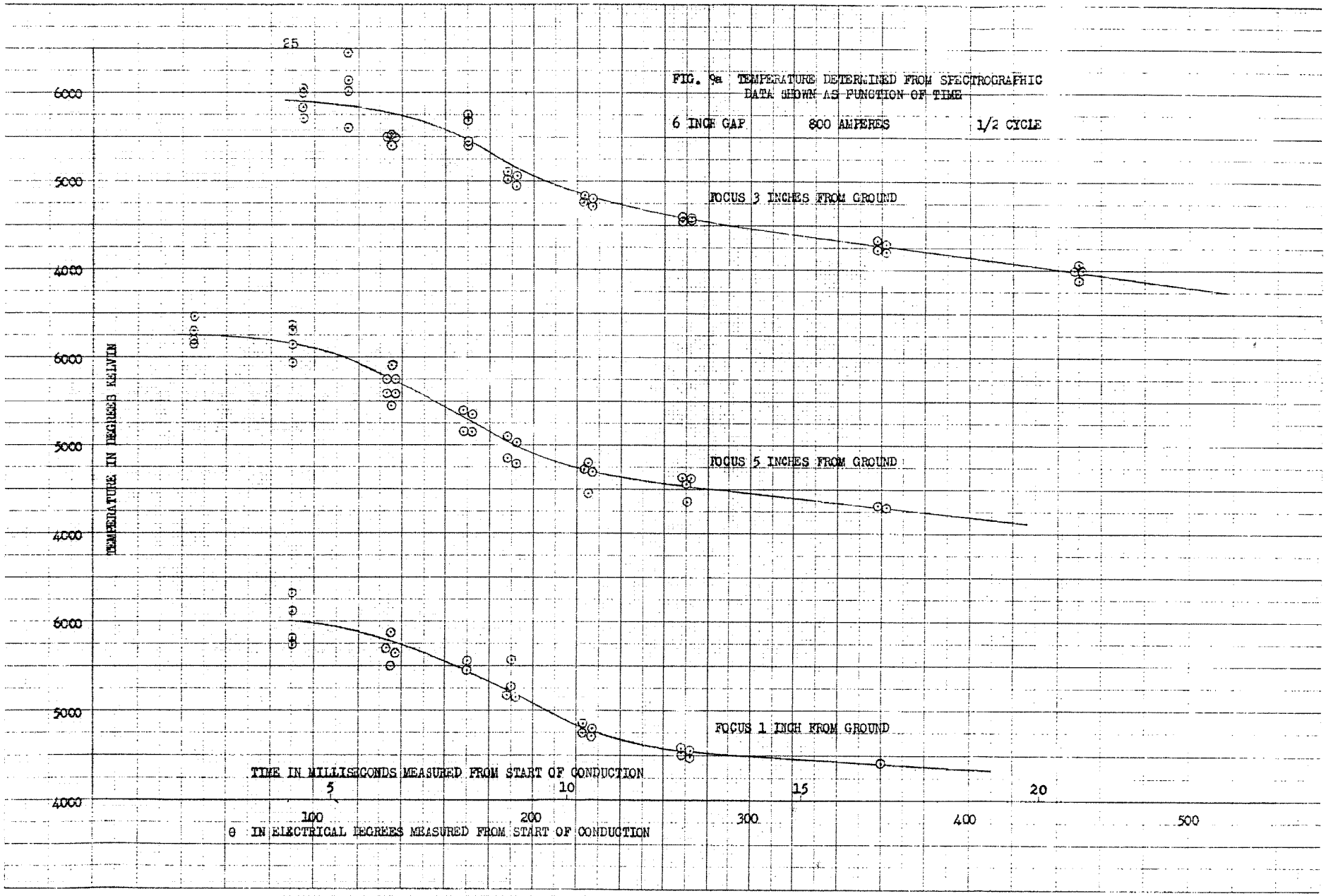
FIG. 9a TEMPERATURE DETERMINED FROM SPECTROGRAPHIC DATA SHOWN AS FUNCTION OF TIME
6 INCH GAP 800 AMPERES 1/2 CYCLE
FOCUS 3 INCHES FROM GROUND
FOCUS 5 INCHES FROM GROUND
FOCUS 1 INCH FROM GROUND
TEMPERATURE IN DEGREES KELVIN
6000
5000
4000
TIME IN MILLISECONDS MEASURED FROM START OF CONDUCTION
5
10
15
20
100
200
300
400
500
θ IN ELECTRICAL DEGREES MEASURED FROM START OF CONDUCTION

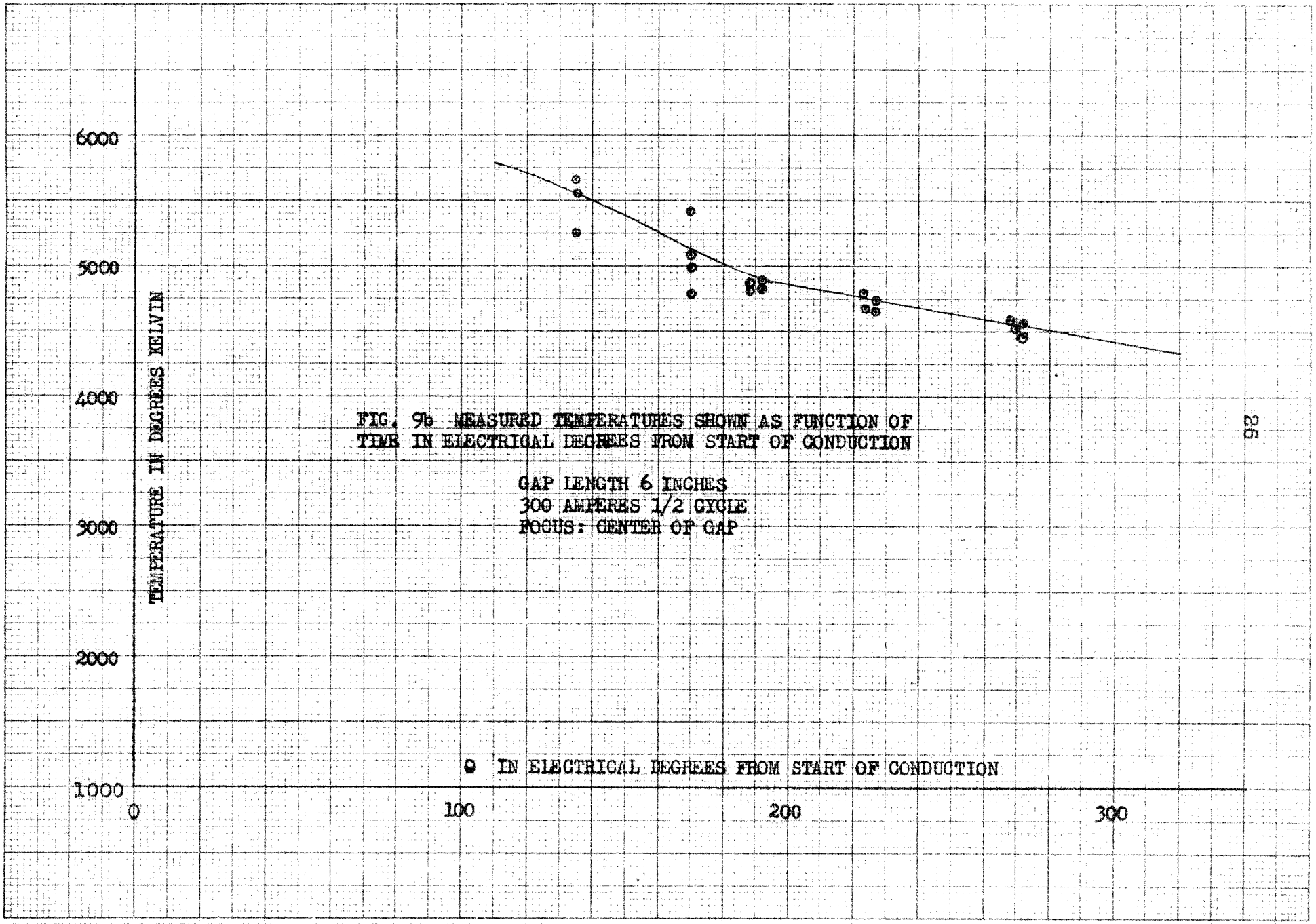

FIG. 9b MEASURED TEMPERATURES SHOWN AS FUNCTION OF TIME IN ELECTRICAL DEGREES FROM START OF CONDUCTION

GAP LENGTH 6 INCHES
300 AMPERES 1/2 CYCLE
FOCUS: CENTER OF GAP

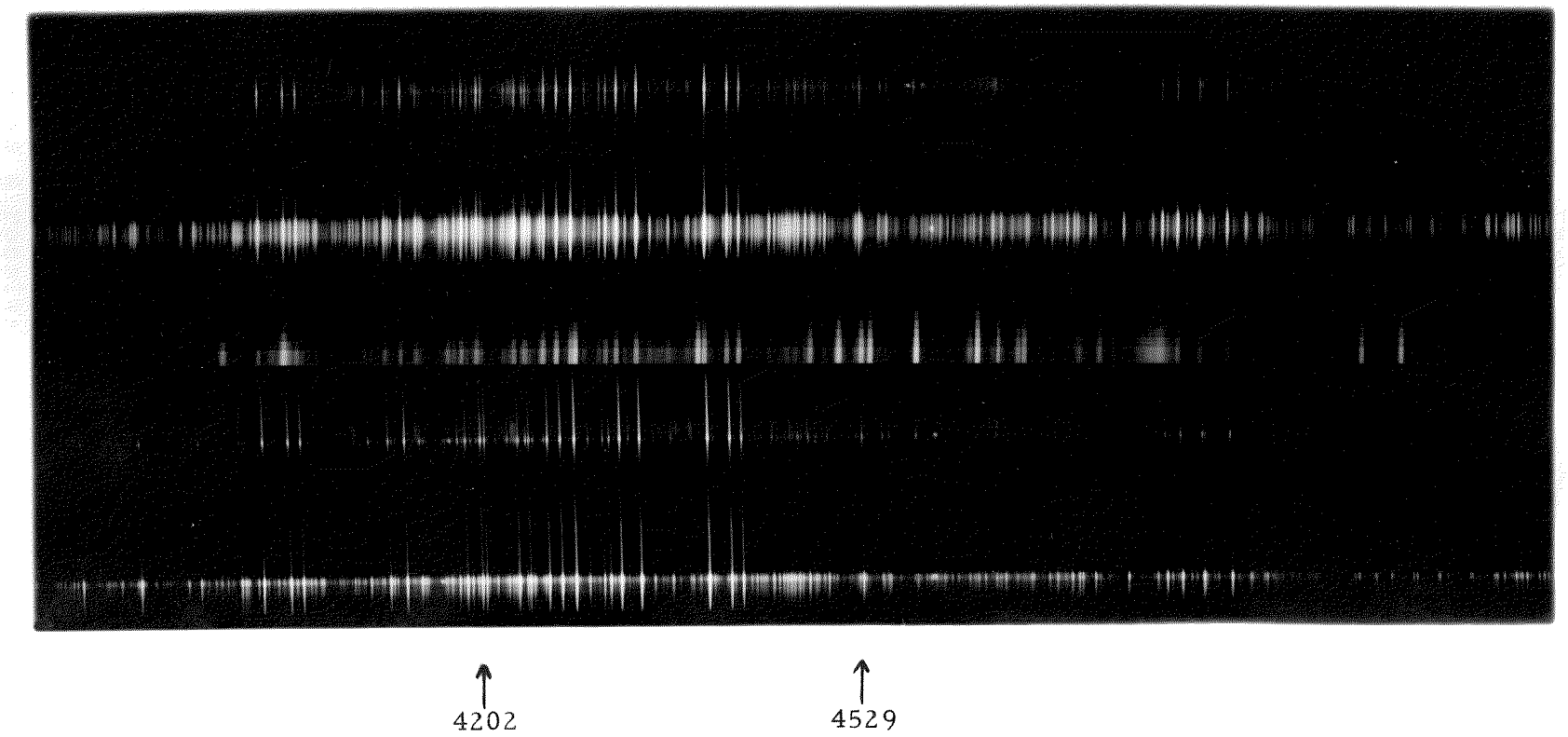

FIG. 10 SPECTROGRAPH PLATE SHOWING CONTINUIM

800 amperes 1/2 cycle $\theta = 90$ eleç. degrees
Focus 1 inch from ground electrode One shot per exposure

Velocity of Sound Measurements

Theory and Technique. The velocity of sound in a gas is inversely proportional to the square root of the gas density and proportional to the square root of pressure;

$$v \propto (P/\rho)^{1/2} \propto T^{1/2}$$

There are limitations to the use of the above expressions. When the sound intensity is very great, the velocity is a function of that intensity. At very high temperature the gas may dissociate so that the velocity as a function of the temperature depends on the degree of dissociation. These factors have been investigated by Suits (10) who used the velocity of sound measurements in arcs as a measure of the arc temperature. The method of Suits was used here to obtain temperature measurements long after current zero.

The technique of Suits can be described briefly as follows. The voltage across a low-current, high-voltage, atmospheric pressure discharge changes abruptly when a sound disturbance passes through the discharge if the sound disturbance has a sufficiently steep front. The theory of the operation of this receiver is not known. A possible explanation could be based on the fact that the voltage across such a high-voltage, low-current, high-pressure discharge varies greatly with pressure. An increase in pressure causes an increase in voltage. Another possible explanation could be that the sound wave disturbs the 'high-field' region near the cathode. Suits used such a discharge as a receiver (microphone). The advantages of

using this receiver are that it can be placed directly in or very near the arc region and that the response is fast. Suits discharged a condenser through a gap in the arc stream to produce the steep front explosion required for the velocity of sound measurement. The difference in time between the condenser discharge and the change in receiver voltage was observed on an oscillograph screen.

This technique was used here to determine densities and temperatures in the arc space after current zero; it could be used at times for which the spectrographic method could not be used. A schematic diagram of the experiment is shown as Fig. 11.

With 2500 volt, 60 cps potential applied to stand-off gap G_2, surge generator No. 1 was fired at the proper phase for subsequent sinusoidal current power follow through gaps G_1 and G_2. Gaps G_5 and G_6 were broken down by the surge generator. Capacitor C_1, charged to 50 kv, discharged through R_1 producing the low-current discharge through receiver gap G_5. The power current flow was limited to 1/2 cycle by bias controls in the ignitron igniter circuit. The voltage of receiver gap G_5 was applied to the vertical plates of a Westinghouse cathode ray oscillograph through a high resistance voltage divider and 15 feet of RG34U cable. The cable capacity and high resistance divider prevented the short time duration, high potential output from surge generator No. 1 from being applied to the oscillograph. At a predetermined time after the first surge generator was

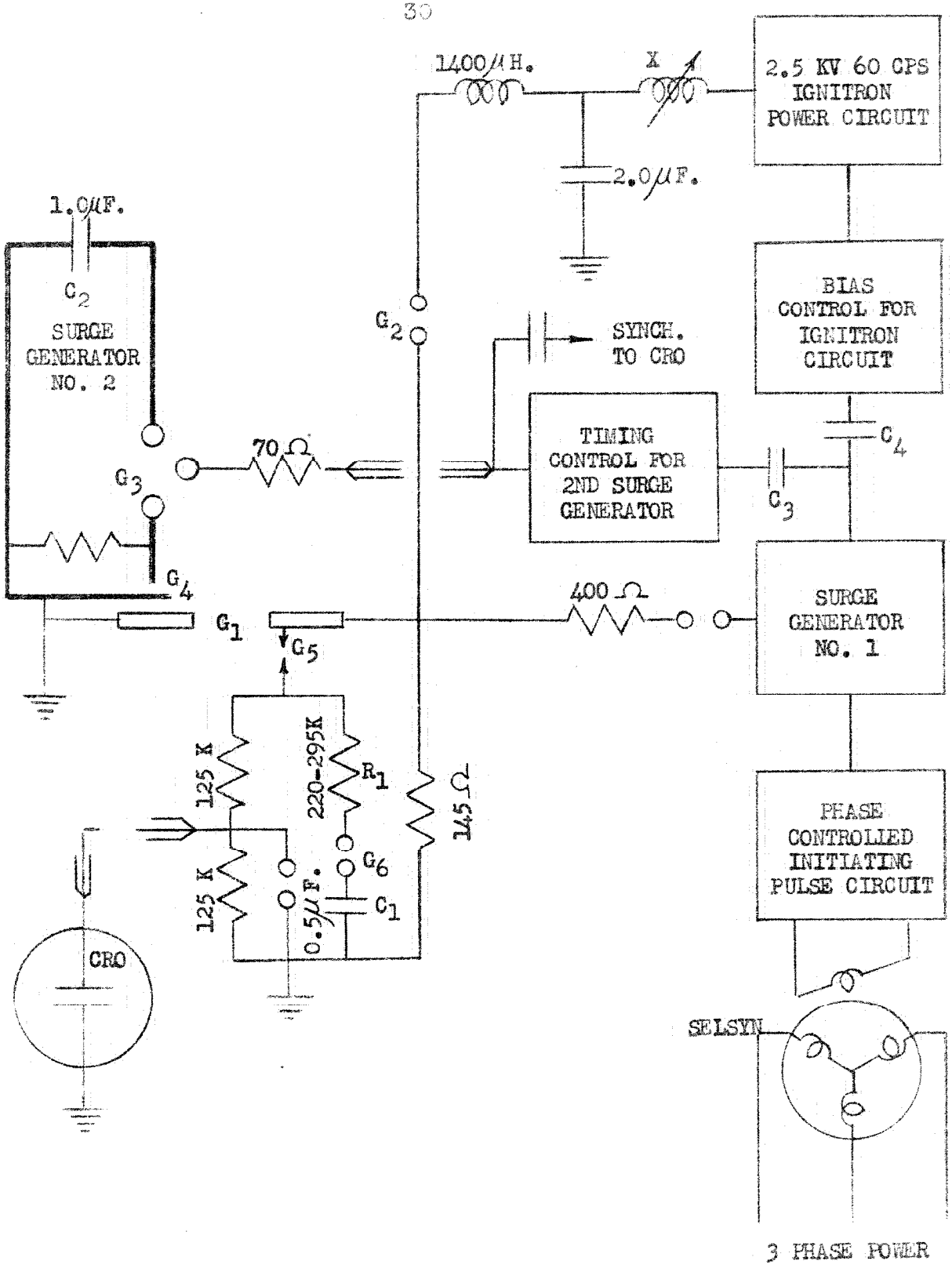

FIG. 11 SCHEMATIC BLOCK DIAGRAM OF SOUND VELOCITY EXPERIMENTS

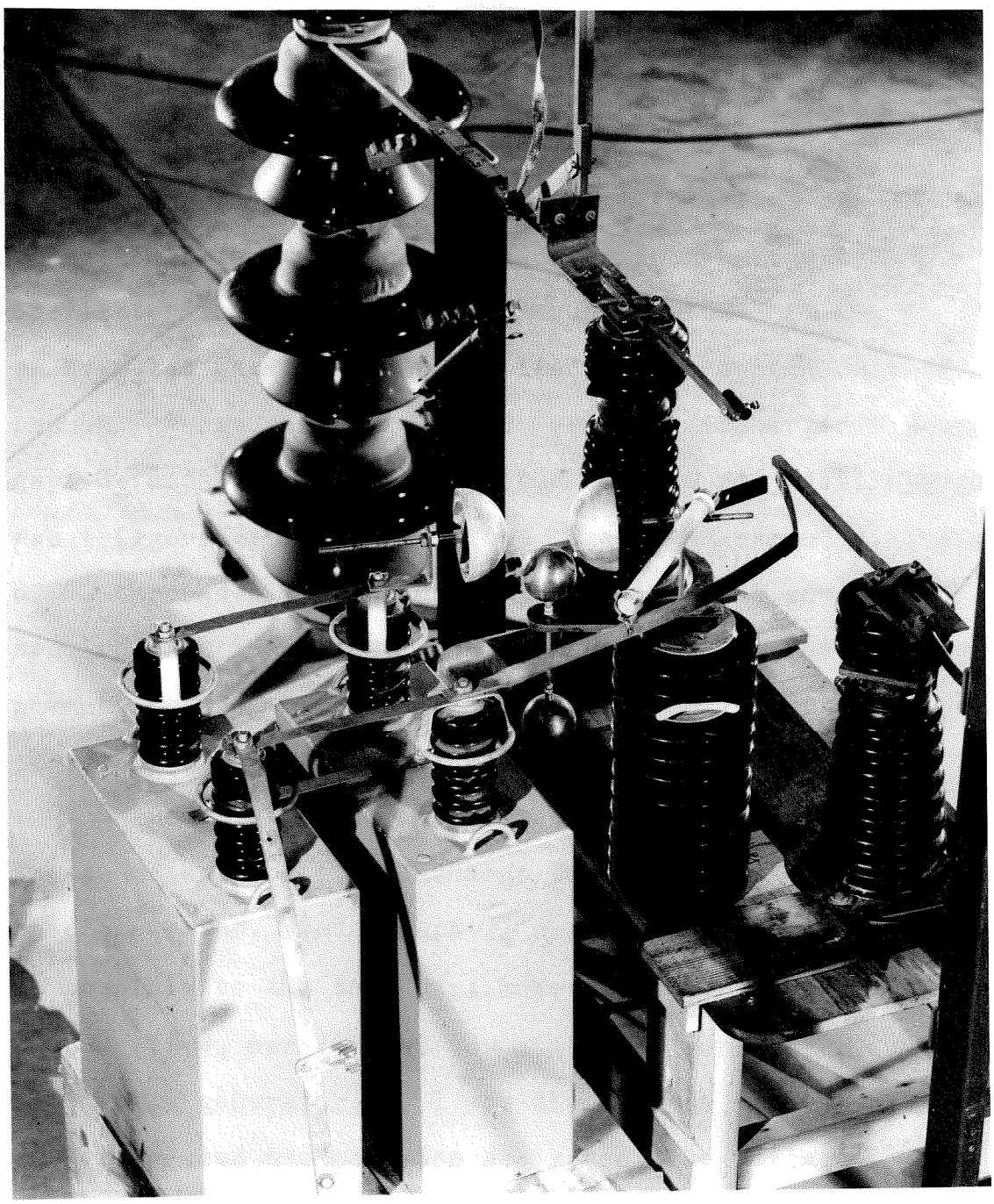

FIG. 12 PHOTOGRAPH OF EQUIPMENT USED FOR SOUND VELOCITY MEASUREMENTS SHOWING SURGE GENERATOR NO. 2, SOUND GAP, TEST GAP, AND RECEIVER GAP.

tripped, the second surge generator was fired. The time delay circuit consisted of a gated ten-stage binary counter which counted cycles of an audio oscillator. The gate was initiated from a pulse picked up from the first surge generator. The time delay was determined by the audio oscillator frequency. After a count of 1024 cycles, a 45 kv pulse was formed and applied to the center ball of gap G_3. Surge generator No. 2 was then discharged through gaps G_3 and G_4. The sweep of the cathode ray oscillograph was triggered at the same time. The high-current discharge of C_2 through gap G_4 produced the steep front sound wave required for the sound velocity measurement. The sound wave then traversed the gap space, and its arrival at the receiver gap could be observed on the oscillograph sweep.

Condenser C_2, 1.0 microfarads, was charged to 90 kv. The inductance of its discharge loop was kept at the minimum possible value. Sound gaps G_4 and G_5 were placed as close as possible to the test gap; however, there were limitations. If G_4 were placed too close, C_2 would be discharged when surge generator No. 1 was discharged. If receiver gap G_5 were placed too near the arc space, the voltage across G_5 would be disturbed by the motion of the gases in the test gap. The receiver gap was placed in a 3/8" I.D. x 5/8" O.D. bakelite tube. The receiver gap was placed 5/8 inch from the end of this tube. This tube was attached to the hot electrode of the test gap. The tube helped shield the receiver gap from the test gap gases. The receiver gap was

7/8 inch from the end of the electrode rod. The receiver gap was 0.07 inches long. The sound gap G_4 was 3/8 inch long. The sound gap was located 1-3/4 inches back from the end of the ground electrode and 1-1/4 inches away.

Because the sound gap and receiver gap could not be placed directly in the test gap, the sound traveled through relatively cold gases at each end of the arc space. With the half-cycle of current maintained at 800 amperes crest, data was taken for gap lengths of 4,5,6,7, and 8 inches. A curve was plotted of sound travel time versus distance traveled. The slope of this curve was taken as inversely proportional to the sound velocity. The end effects were compensated for in this way.

When the sound intensity is very great, the velocity of sound is a function of that intensity. Such abnormal velocities were observed. These abnormal velocities were found to be dissipated after 4 inches of travel from the sound gap. After 6 inches of travel the velocity was measured, without the power current discharge, and found to be 13.2 inches per millisecond within 2%. The abnormal velocity near the sound gap could be, and was, included as part of the end effects.

Results of the Velocity of Sound Measurements. A typical set of test oscillograms is shown as Fig. 13. The oscillograph sensitivity is 250 x 2 volts per centimeter. The results of scaling such a set of oscillograms are plotted on Fig. 14. Considerable spread can be observed in

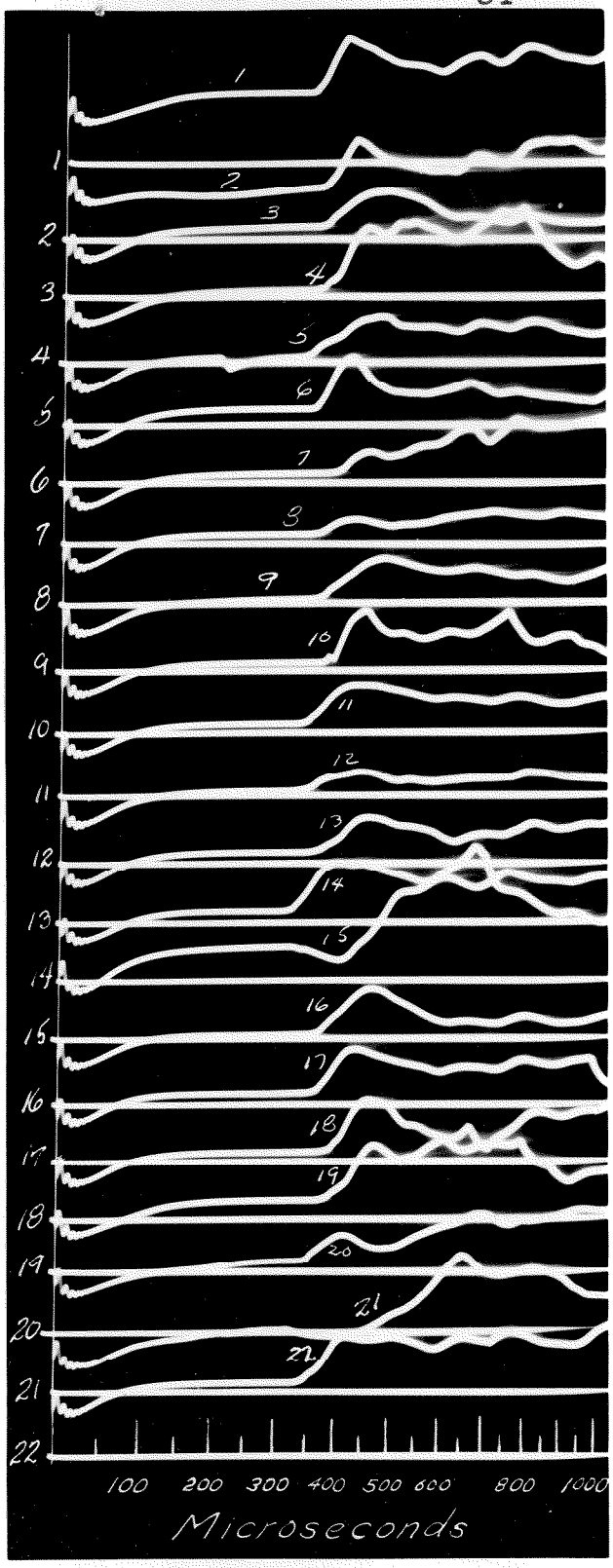

TEST GAP LENGTH
4 INCHES

POWER CURRENT
800 AMPERES - 1/2 CYCLE

RECOVERY TIME DELAY
51.9 MILLISEC.

FIG. 13 TYPICAL OSCILLOGRAMS SHOWING ARRIVAL OF SOUND WAVE AT THE RECEIVER GAP.

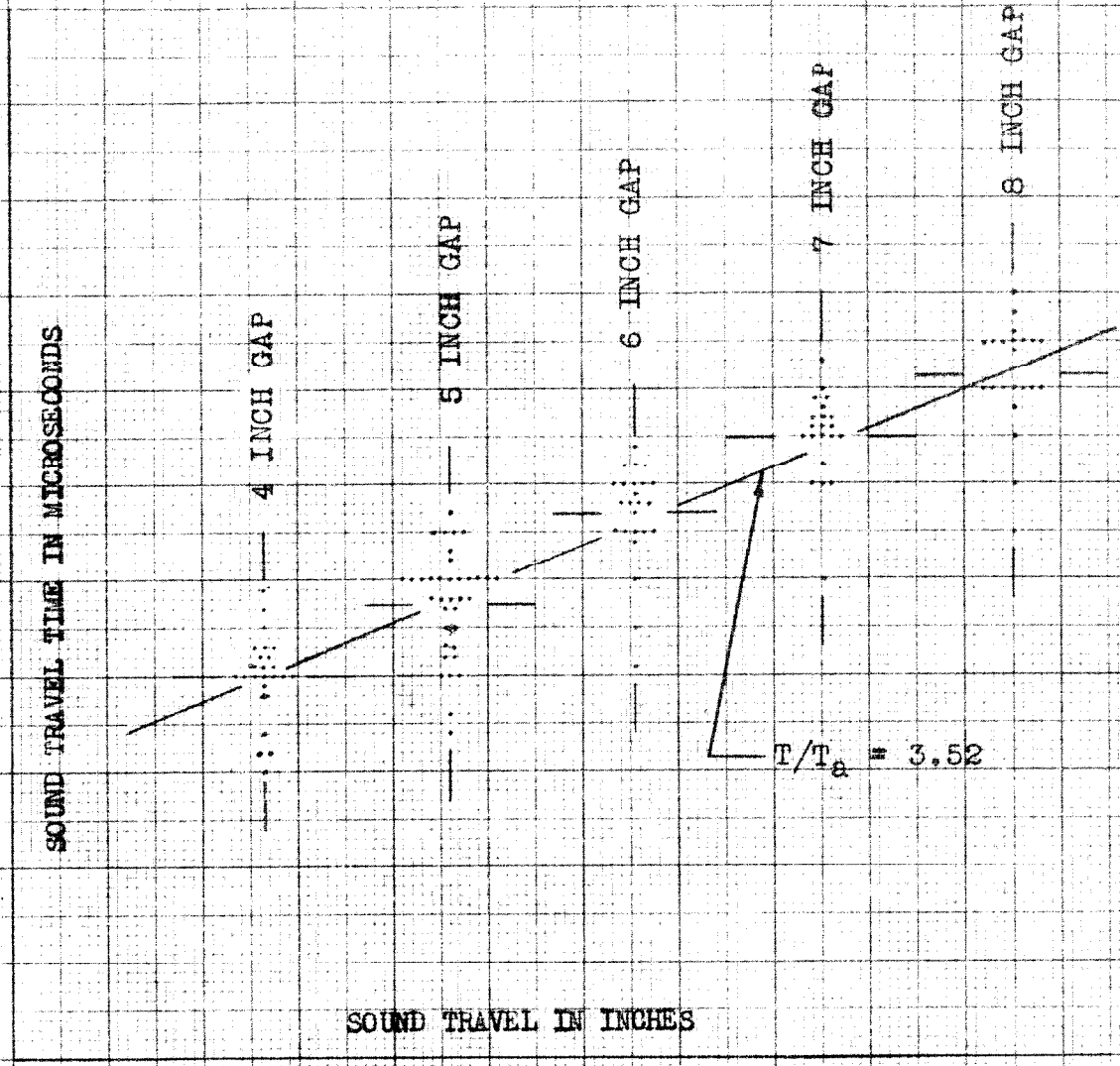

FIG. 14 SOUND TRAVEL TIME VERSUS TRAVEL DISTANCE

RECOVERY TIME DELAY 17.3 MILLISECONDS
800 AMPERES 1/2 CYCLE

the points plotted. This spread of points is not due to the test technique but to the condition and configuration of the arc space gases. This was checked by tests with no arc discharge. Then, the observed spread of points was less than 10 microseconds while the velocity was measured within 2% of the accepted value. This velocity was measured 6 to 12 inches from the sound gap after the abnormal velocities had dissipated. By working with the slope of the time versus distance curve, compensation was supplied for the end effects including these abnormal velocities. Suits (10) shows that these shock waves tend to be refracted out of the region of hot gases.

Representative values of temperature and density were obtained by drawing a curve through the average time of sound travel for each gap length. On Fig. 14 all of the points should be plotted at distances marked by the heavy vertical lines. The average times are indicated by the heavy horizontal lines. The velocity of sound was taken as inversely proportional to the slope of the straight line drawn through these points.

It should be understood that the gases of the arc space are by no means homogeneous in density. Values of density exist in the arc space which are greater than and less than the value obtained by this method. Indeed, all effects that can be mentioned tend to lower the estimate of temperature and increase the estimate of density obtained in this way. It should be emphasized that no two arcs are

the same. Ellis obtained high speed motion pictures of many arcs which show much variation of the luminous cloud shape. The tortuous expansion of the arc leaves the hot gases in very irregular shapes which may or may not lie along the direction of sound travel for a particular shot. Studies of the pictures of Ellis indicate that the sound in traversing the gap may pass through some regions of gas which have been heated very little. Now as the space is not homogeneous in density, slower velocities are emphasized when the average is determined. If the sound in traversing 8 inches travels 4 inches at 13.3 inches/millisecond and 4 inches at 40 inches/millisecond, the average velocity is 8 inches in 0.4 milliseconds - 20 inches/millisecond which is nearer 13.3 than 40. The hot gases refract the sound waves and slope the front of the wave so that the earliest disturbance at the receiver may not be recorded. Such effects all indicate that there are regions in the arc space at temperatures greater than those determined by this method.

At one value of time delay, many shots were taken in the hope that the distribution of points (minimum travel times) would lead to a better estimate of the highest temperatures in the region. Although the results were inconclusive, they are shown as Fig. 15.

The results of this study are listed in the following table, Table 2.

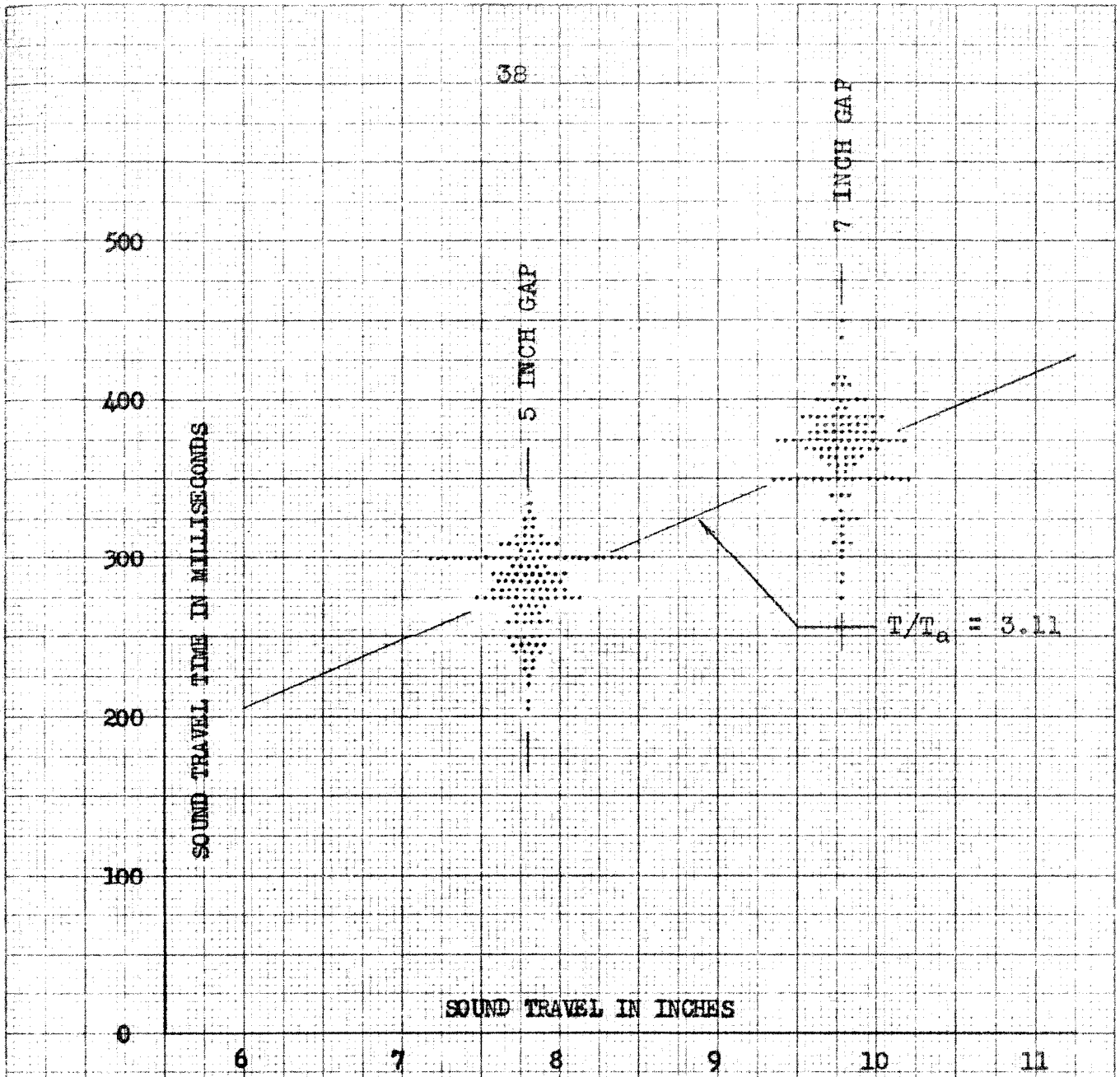

FIG. 15 SOUND TRAVEL TIME VERSUS TRAVEL DISTANCE

RECOVERY TIME DELAY 32.6 MILLISECONDS
800 AMPERES 1/2 CYCLE

Results of the Sound Velocity Investigation

Audio Oscillator Frequency Kilocycles	Recovery Time Delay Milliseconds	$\frac{\rho_a}{\rho} = \frac{T}{T_a}$
5	196.5	1.38
8	119.7	2.02
12	77.0	2.41
25	32.6	3.11
40	17.3	3.52

Application of Results to Dielectric Recovery

Effect of Air Density on Recovery Dielectric Strength. When the arc is initiated, temperatures in the core are very high due to electrical energy converted into heat in the arc. Immediately after the arc is initiated, pressure in and around the arc core is very great. The hot gas of the arc region expands until the region is at atmospheric pressure. These readjustments and changes in pressure should occur with velocities of the order of 1.1 feet/millisecond, the speed of sound. One would then expect the pressure to be atmospheric pressure after a few milliseconds of conduction and during the recovery period. Then the air density is given by

$$\rho = \rho_a \, Ta/T \tag{5}$$

where ρ_a and T_a are the density and temperature of the air at normal room temperature.*

Paschen's Law roughly governs practically all spark-breakdown phenomena. In all of the usual derivations of Paschen's Law the essential meaning of (Pd) in sparking lies in the number of molecules per centimeter length of electron travel that are encountered by the electron. This number depends primarily on the gas density rather than the gas pressure. Paschen's Law should be stated that the spark-breakdown voltage is a function of (ρd) rather than (Pd). The relative variation of breakdown with density

---

* The effect of gas dissociation on this equation is discussed later.

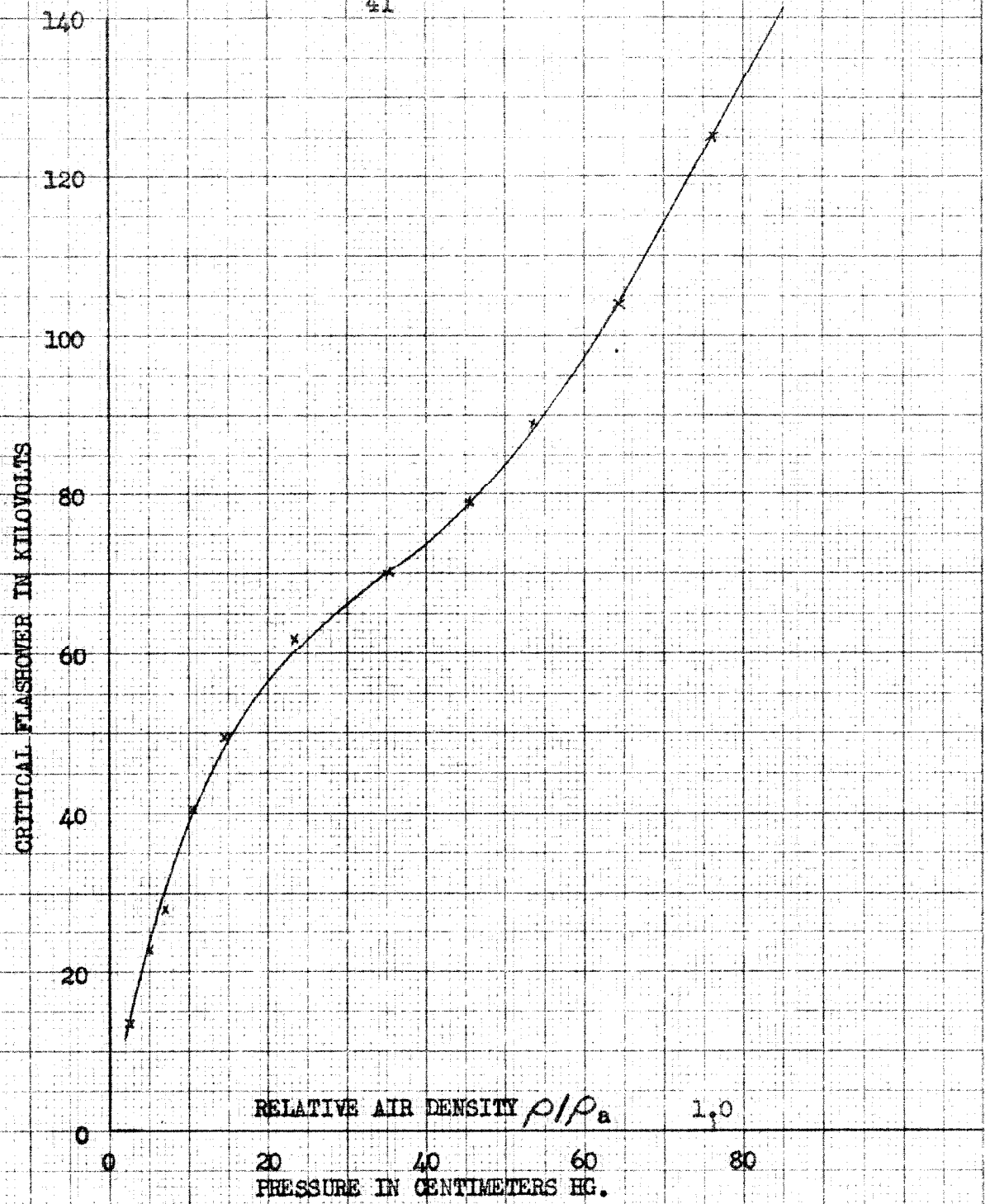

FIG. 16 BREAKDOWN VOLTAGE AS A FUNCTION OF RELATIVE AIR DENSITY OR OF PRESSURE AT ROOM TEMPERATURE OF A 6 INCH ROD GAP WITH APPLIED POSITIVE 1 1/2 x 40 MICROSECOND PULSE VOLTAGE

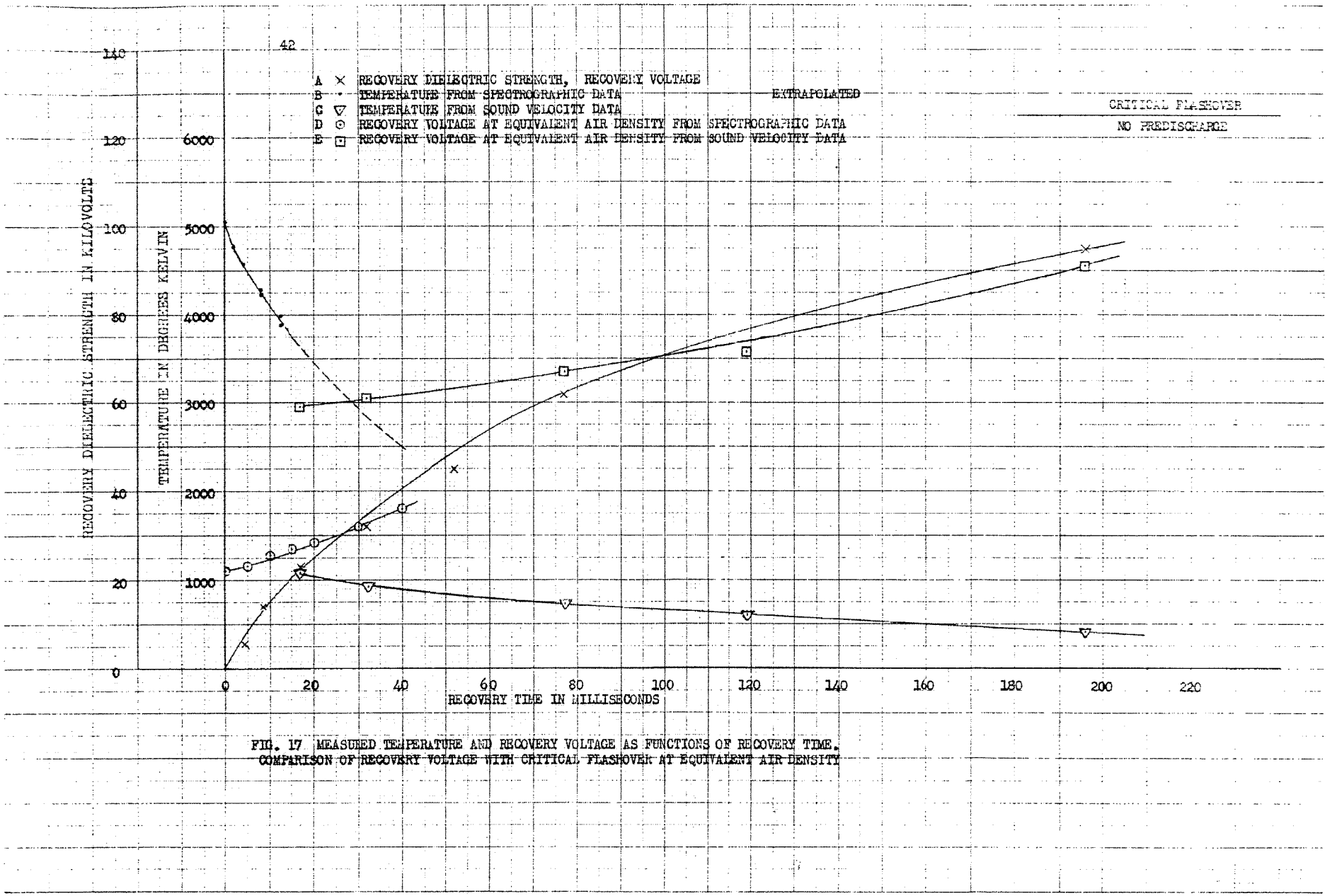

FIG. 17 MEASURED TEMPERATURE AND RECOVERY VOLTAGE AS FUNCTIONS OF RECOVERY TIME. COMPARISON OF RECOVERY VOLTAGE WITH CRITICAL FLASHOVER AT EQUIVALENT AIR DENSITY

can be determined by varying the pressure at constant temperature. The variation so determined can be used when the temperature varies at constant pressure.

Fig. 16 shows a curve of critical flashover of a 6 inch rod gap plotted as a function of pressure at room temperature. The abscissa can be plotted as relative density (ρ/ρ_a) where $(\rho/\rho_a) = 1.0$ corresponds to 760 mm. pressure, room temperature. This curve was obtained in the laboratory from tests using a positive 1 1/2 x 40 microsecond impulse voltage. The 6 inch rod gap was placed in an evacuated chamber 18 inches high and 18 inches in diameter.

Fig. 17 shows the variation of temperature as determined by the average velocity of sound and by spectrographic measurements (extrapolated). The recovery voltages, which would exist if all factors except the reduced air density were negligible, are also plotted on Fig. 17. These curves were obtained from the equivalent air densities, as given by Eq. 5, and the curve of breakdown voltage versus density. On the same figure, these curves are compared with the actual dielectric recovery values as determined by the two surge technique of McCann, Conner, and Ellis. The curve is from data reported by Ellis (7). Since the spectrographic measurements indicate the temperature of the hottest portions of the arc space, and since the cooler portions influence the average velocity more than the hot portions; the curves indicate that after something like

60 milliseconds the low recovery strength is accounted for entirely by the density of the arc space gases. Before this time, the low density represents a major factor in reducing the recovery voltage; however, some other mechanism must be active.

There is evidence of there being other factors important to the recovery process. Firstly, the reduced air density can account for most of the reduction in dielectric strength but not all. The critical spark breakdown of the 6 inch rod gap for the gas density corresponding to 5000° K. at atmospheric pressure is 21 kv. Immediately after current zero the dielectric strength increases from a value of the order of the arc burning voltage. For a recovery time delay of 4.5 milliseconds McCann, Conner, and Ellis measured a recovery strength of 5 kv. Secondly, there are the slow breakdowns or 'long-tail' flashovers reported by McCann, Conner, and Ellis. Fig. 18 shows typical oscillograms of flashovers and full waves at various recovery time delays from tests performed by Ellis. These oscillograms are all from tests on a 6 inch gap with power current of 800 amperes, 1/2 cycle. The 'long-tail' flashovers were observed on all tests with recovery time delays of 32 milliseconds and less. Some were observed on the shots of 52 milliseconds time delay. In general, as the recovery time delay increased, the length of tail decreased.

Studies of the effect of temperature, other than the effect of reduced air density, on the ionizing coefficients

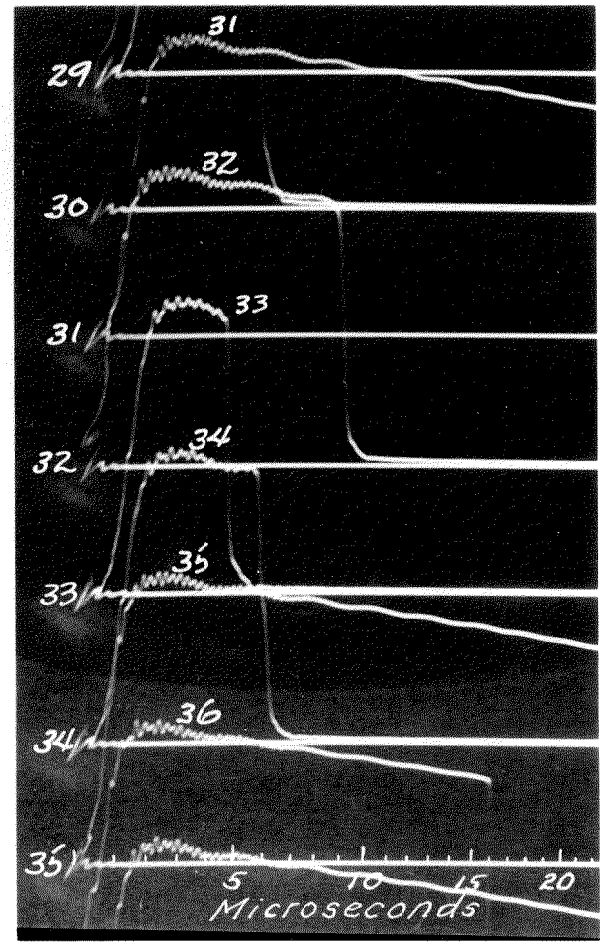

DELAY 77.0 MILLISEC.
SENSITIVITY 16.5 KV/cm

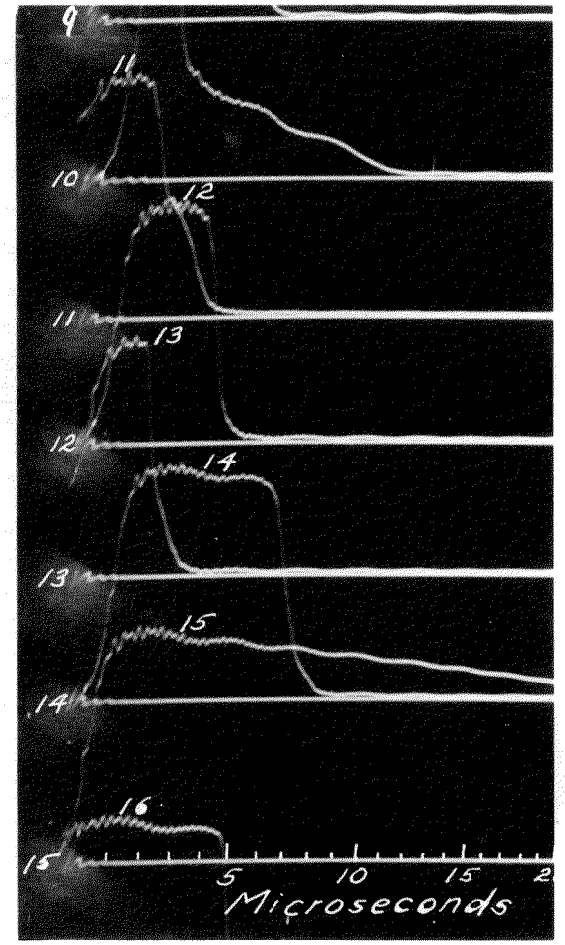

DELAY 52.0 MILLISEC.
SENSITIVITY 19.6 KV/cm

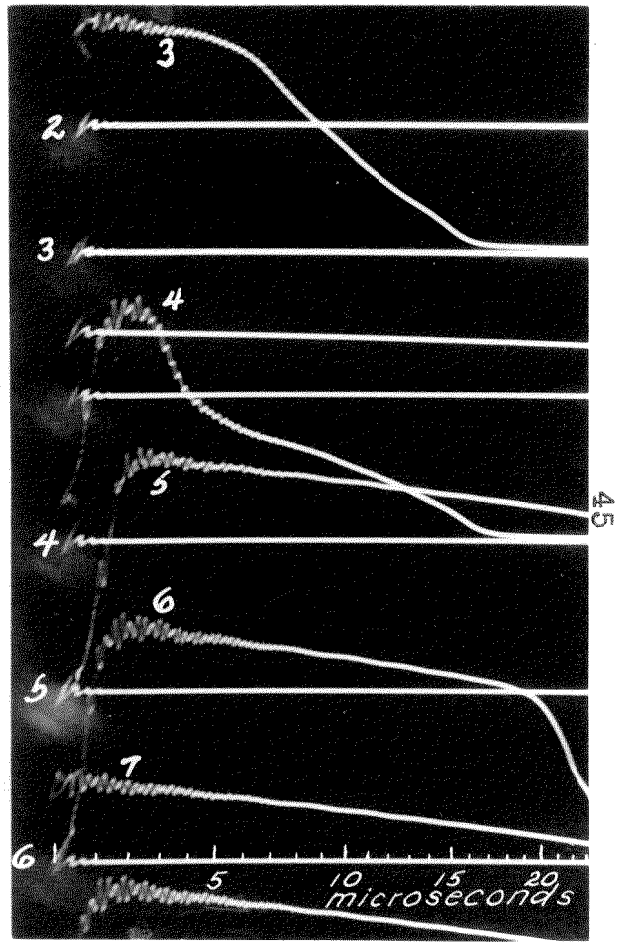

DELAY 32.0 MILLISEC.
SENSITIVITY 9.9 KV/cm

FIG. 18 ILLUSTRATION OF VARIATION OF FLASH-OVER TAILS WITH RECOVERY TIME DELAY

of the Townsend sparking theory indicate that the dielectric strength shortly after current zero is not given by this theory. (See Loeb (16) for a discussion of the Townsend theory.) One might think that the presence of iron vapor would influence the ionizing coefficients as the ionization potential of iron is relatively low; however, calculations of Suits (10) showing that the metallic vapor pressure in arcs is only of the order of 10^{-6} atmospheres invalidate this hypothesis. The effect of temperature on the first ionizing coefficient is discussed in more detail in Appendix B.

The spark has been defined "as an unstable and discontinuous occurrence marking the transition from one more or less stable condition of current between electrodes in a gas to another one." The 'long-tail' flashovers are not of this discontinuous nature. After considerable time delay, the discontinuous spark appears; then the dielectric strength is accounted for entirely by the reduced air density. The change in the breakdown 'long-tails' can be noted as the purely sparking condition is approached. Evidently the recovery dielectric strength depends on both the gas density and the residual ion density in the gap. An acceptable recovery criterion due to Slepian is given below. It is suggested here that the recovery voltage is determined by this criterion unless the value given by this criterion is greater than the sparking potential of the gas at the existing gas density.

The Recovery Criterion of Slepian and the Effect of the Residual Ions in the Gap. After the arc has extinguished, the gases of the arc space still constitute a conductive region due to the residual ions. There should be some critical voltage, for each instant after current zero, which is required to maintain conduction. In the arc itself, the conductive state due to the high population of ions is maintained by thermal ionization; the thermal energy is obtained from the conversion of electrical energy into heat in the arc. The average molecular energy is much less than the ionization potential; however, the collisions are so frequent that those molecules that do have sufficient energy produce ionization. One may refer here to the equation of Saha which gives the degree of ionization as a function of temperature for a gas in equilibrium. This suggests a criterion for the critical voltage mentioned above.

Consider a region of hot ionized gas in the arc space with a thermal energy content per unit volume w. With no applied field, the gas cools, and the ion density decreases due to recombination and diffusion. If an electric field is applied, the resulting flow of ions constitutes conduction current. Electrical energy is then converted into heat in the gas. If the electrical power input to the gap region is more than sufficient to supply the losses by convection, conduction, and radiation; the thermal energy increases. The temperature thus increases with a resulting increase in

ionization. The increase in ion density with the sustained field results in an increased power input with a subsequent rise in temperature, etc. This instability results in the reestablishment of the arc. A field that is sufficient to re-establish the arc can be obtained from

$$(6) \qquad p_e \geqslant dw/dt)_o$$

where p_e is the electrical power input per unit volume and $dw/dt)_o$ is the rate of loss of thermal energy per unit volume by conduction, convection, and radiation at current zero.

The power input to the gap space from the electrical circuit is

$$p_e = \vec{E} \cdot \vec{J}$$

or simply

$$(7) \qquad p_e = X(n_+ eK_+ X + n_- eK_- X)$$

where X is the field intensity, e is the electron or ion charge, n is the ion density, and K is the ion mobility.

At the temperatures existing in the arc space soon after current zero, electron attachment and negative ion formation is highly improbable. Since electron mobility is much greater than ion mobility, Eq. 7 in Eq. 6 gives

$$(8) \qquad X^2 \, neK_e \geqslant dw/dt)_o$$

Loeb (16) gives the Compton electron mobility equation in convenient form as

$$(9) \qquad K_e = \frac{1.825 \times 10^8 \lambda_o \, (760/P)(T/273)(300)}{\left\{1 + \left[1 + 5.71 \times 10^{11} M_o \lambda_o{}^2 300^2 (X/P)^2\right] 1/2\right\} 1/2}$$

where λ_o is the electron mean free path at 273° K and 760 mm Hg., M_o is the gas molecular weight, P is the pressure, and X is the field strength in esu. If P = 760, λ_o = 5.64 x 10^{-5} cm., and M_o = 20,*

$$(10) \qquad K_e = \frac{1.87 \times 10^5 \, T^{1/2}}{\left\{1 + \left[1 + 5.67 \times 10^3 \, X^{\,2}\right]^{1/2}\right\}^{1/2}} \text{ esu}$$

For $5.67 \times 10^3 \, X^{\,2} \ggg 1$,

$$(11) \qquad K_e = 2.17 \times 10^4 \, T^{1/2} \, X^{-1/2}$$

The rate of loss of energy per cubic centimeter is estimated in Appendix A as

$$(12) \qquad (dw/dt)_o = (dw/dT)(dT/dt)_o = 1.87 \times 10^8 \text{ cgs}$$

If this value is substituted in Eq. 8, there results

$$(13) \qquad X = 4.02 \times 10^7 \left(\frac{5000}{T}\right)^{1/3} \left(\frac{1}{n}\right)^{2/3}$$

for the dielectric recovery field strength at short time intervals after current zero. Since there is no information available which can be used in computing the ion density as a function of time, Eq. 13 can not be used for computing recovery dielectric strengths; however, the equation can be used to give information regarding the ion density. The order of magnitude of the electron density and its variation can be computed from Eq. 13, the dielectric recovery voltage,

---

* Much of the air is dissociated at these temperatures. The value K_e is dependent on M_o only as $M_o^{-1/4}$

and the extrapolated temperature curves of Fig. 17. The results of this calculation are given in the table below and plotted on Fig. 18. The average field strength was used for X.

Table 3

The Electron Density as a Function of Time after Current Zero

t	X	T	n
Milliseconds	esu	^{o}K	cc^{-1}
10	3.34	4100	4.60×10^{10}
20	5.62	3450	2.30×10^{10}
30	7.34	2950	1.68×10^{10}
40	8.90	2500	1.36×10^{10}

The loss of ion or electron density by recombination is determined by the equation

$$dn/dt = -\alpha n^2$$

and its solution

$$n = n_o/(1 - \alpha n_o t)$$

If n_o is very large, then after appreciable time

$$n = 1/\alpha t$$

The electron density determined above in Table 3 varies very approximately as $1/\alpha t$ where $\alpha = 2.0 \times 10^{-9}$. As stated before, electron attachment to neutral atoms and subsequent recombination with positive ions ($\alpha \doteq 10^{-6}$ for this recombination process) is not likely to occur at very high temperature. The recombination during the recovery period is electron recombination which is also an improbable process as three

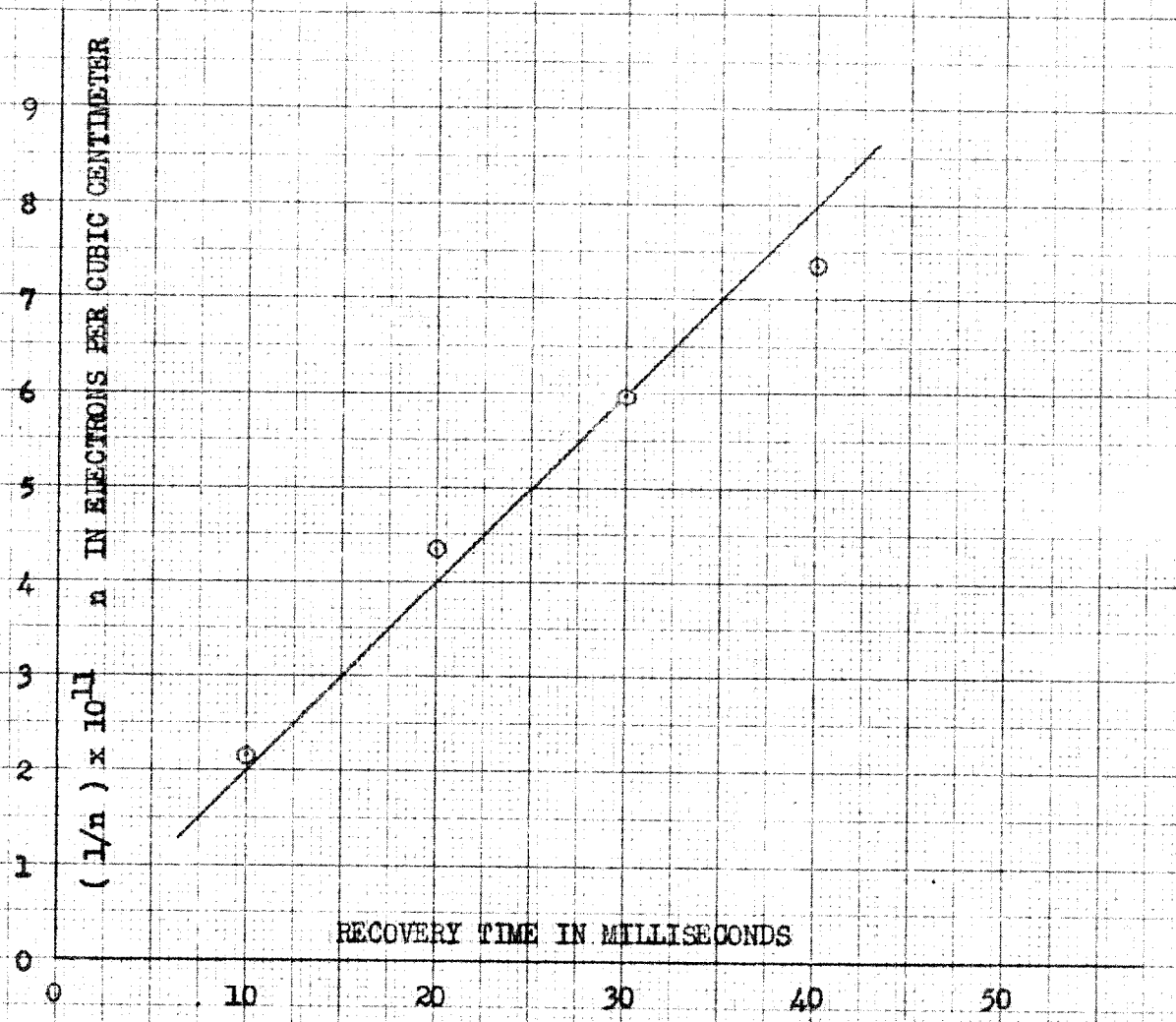

FIG. 19 VARIATION OF ELECTRON DENSITY WITH TIME AFTER CURRENT ZERO

body collisions are required. Electron recombination coefficients of $\alpha = 10^{-10}$ have been reported by Kenty (17) and Mohler (18). These values were found for electron recombination with metallic ions at low vapor pressures. The value of α should be a function of the pressure as well as the partial pressure of other gases present as the probability of three body collisions increases with the pressure. Values of α for electron recombination with non-metallic ions of the order of $\alpha = 10^{-8}$ have been reported (19).

From the data available, it may be concluded that the variation of electron density is due to recombination, and $n = 1/\alpha t$ may be substituted in Eq. 13. At lower temperatures electron attachment is possible and the electrons disappear some 1000 times as fast. The possibility that the variation of ion density computed above is due to the diffusion of ions from the open arc space is investigated in Appendix C. The study of Appendix C supports the conclusion that the variation is due to electron volume recombination.

If in Eq. 8 the arc burning voltage is taken as 300 volts or 1 esu, the losses are taken as 1.87×10^{8} ergs/second/cc, and K_e is computed from Eq. 9; the electron density in the arc can be calculated and is $n_o = 6.5 \times 10^{12}$ per cc. This value agrees with values estimated elsewheres; Loeb (16) refers to values from 0.6×10^{12} per cc to $10^{13} - 10^{14}$ per cc.

Conclusion

Evidence has been given that the recovery of dielectric strength of arc spaces after conduction of power frequency currents of the order of 800 amperes depends on the variation of both the density of the gas and the degree of ionization. After some 60 milliseconds of recovery time for the 800 ampere, 1/2 cycle, 6 inch arc the dielectric strength can be accounted for solely by the gas density. Throughout the recovery period the low gas density is a major factor contributing to the low dielectric strength. Residual ions effect a reduction in the strength for recovery times shorter than 60 milliseconds. The reduction in dielectric strength due to the residual ions in the gap depends on a race between the deionizing agent, recombination, and the ionizing agent, the applied field. Now, a low value of applied voltage can also act as a deionizing agent by removal of the ions; therefore, one may speculate that, at short times after current zero, the measured dielectric strengths should also be a function of the wave-form of the applied voltage. The data of McCann, Conner, and Ellis were taken with a 1-1/2 x 40 microsecond test surge. It is estimated that for the critical voltages they observed that the time for an electron to traverse the gap is of the order of 3 microseconds.

An analysis for estimating the variation of temperature with time has not been included due to a lack of knowledge of how much of the energy stored in the arc space is

converted to translational kinetic energy as the temperature decays. Such an analysis should include the variation of the air thermal conductivity with temperature; the conductivity varies approximately as the square root of the temperature for constant pressure. An upper limit for an estimation of the distance that the hot gases rise out of the gap due to buoyancy or convection can be obtained from $s = 1/2\ gt^2$ where t is the time and g is the acceleration of gravity.

Appendix A

Estimation of the Energy Content of the Arc Space

In order to apply Slepian's criterion to the recovery of a long gap after current conduction, an estimation of the energy loss per cubic centimeter per second is required. During the conduction period, the gases of the arc space are heated. The gases expand; and, at the high temperatures that exist, the gases dissociate. The calculations of this appendix determine the energy content per cubic centimeter as a function of the gas temperature including

(1) The translational kinetic energy of N_2, O_2, N and O.

(2) The energy of rotation and vibration of N_2 and O_2.

(3) The work of expansion.

The data used for the computation include the specific heats of N_2 and O_2 as given in the International Critical Tables. These are

$$C_P = 6.98 + 1.51 \times 10^{-4} T + 6.7 \times 10^{-8} T^2$$

$$C_P = 6.732 + 2.88 \times 10^{-4} T + 5.3 \times 10^{-8} T^2 \quad \text{cal/mole/}^{o}\text{K}$$

for N_2 and O_2, respectively, where T is in degrees Kelvin. Above 3000° K information was taken from a paper of Suits and Poritzky giving C_P of N_2 and O_2 and the degree of dissociation of oxygen and nitrogen as a function of temperature of the air mixture at atmospheric pressure (20). The

information of Suits and Poritzky is given in the following table. P_o represents the partial pressure of O as a fraction of an atmosphere.

All of the energies computed are the energies above that required at 300° K. The average heat content per particle of N_2 and O_2 is given by

$$w_h = \frac{4.19 \times 10^7}{N_o} \int_{300} C_p dT - kT \quad \text{ergs}$$

where N_o is Avogadro's number, k is Boltzman's constant, and w_h is in ergs. The integrals were taken graphically from the curves shown as Fig. 20. The average heat content per particle of N and O is given by

$$w_h = \frac{3}{2} kT$$

The heat input to account for dissociation of the dissociated particles is

$$w_d = 1.6 \times 10^{-12} \left(\frac{V_d}{2}\right)$$

ergs per particle of N or O where V_d is the potential of dissociation in electron volts. The total heat content per cubic centimeter is then

$$w_T = 2.705 \times 10^{19} \left(\frac{273}{T}\right) \left\{ \sum_j w_{hj} P_j + \frac{1.6 \times 10^{-12}}{2} \sum_i V_{di} P_i \right\} \text{ergs/cc}$$

Here $2.705 \times 10^{19} \left(\frac{273}{T}\right) P_j$ gives the number of particles of gas j per cubic centimeter where P_j is its partial pressure in atmospheres. Lochschmidt's number is 2.705×10^{19}. The first sum is taken over all four gases while the second is taken

over N and O only.

The results of the above calculations are given in Table 5. Also included is the energy required for the work of expansion

$$w_P = P \Delta V = P \left(1 - \frac{300}{T}\right)$$

for each cubic centimeter at temperature T where P is 1.013×10^6 dynes/ cm^2. These quantities are plotted as Fig. 21.

At 5000° K, the slope of $w_P + w_T$ is 1.87×10^3 ergs/cc/$^\circ$K. Immediately after current zero, the temperature of the arc space was observed to change approximately 10^5 degrees/ second. The power input required to maintain conduction can be estimated as

$$\left(\frac{dw}{dt}\right)_o = 1.87 \times 10^8 \quad \text{ergs/sec./cc.}$$

The total amount of energy supplied to the 800 ampere, 1/2 cycle arc discharge is 1,925 joules. This value was determined by graphically integrating

$$W = \int p\,dt = \int i v_g\,dt$$

where the values of current i and gap voltage were taken from oscillograms.

Table 4

Variation of Specific Heat of N_2 and O_2 and Degree of Dissociation of Air at Atmospheric Pressure as Functions of Temperature

T	CP_{N2}	CP_{O2}	P_{N2}	P_N	P_{O2}	P_O
^oK	cal/mole					
3000	8.86	9.11	0.767	0.0005	0.182	0.0506
3500	8.93	9.22	0.717	0.0038	0.108	0.1707
4000	8.99	9.33	0.657	0.0214	0.0377	0.2835
4500	9.04	9.44	0.593	0.077	0.0087	0.322
5000	9.08	9.55	0.489	0.1975	0.0019	0.312
5500			0.340	0.38	0.00	0.28
6000			0.190	0.56	0.00	0.25

Table 5

Energy Content per Cubic Centimeter of Air at Temperature T, Atmospheric Pressure Above That Energy at 300^oK

T	w_T	w_P	$w_P + w_T$
^oK	Joules/cc	Joules/cc	Joules/cc
300	0.00	0.00	0.0
500	0.0394	0.0405	0.0799
1000	0.1372	0.071	0.2082
1500	0.1871	0.081	0.2681
2000	0.2103	0.086	0.296
2500	0.2272	0.0892	0.316
3000	0.2894	0.0913	0.371
3500	0.3958	0.0925	0.488
4000	0.4737	0.0938	0.568
4500	0.5355	0.0945	0.630
5000	0.6177	0.0952	0.7129
5500	0.7197	0.0959	0.816
6000	0.8151	0.0963	0.911

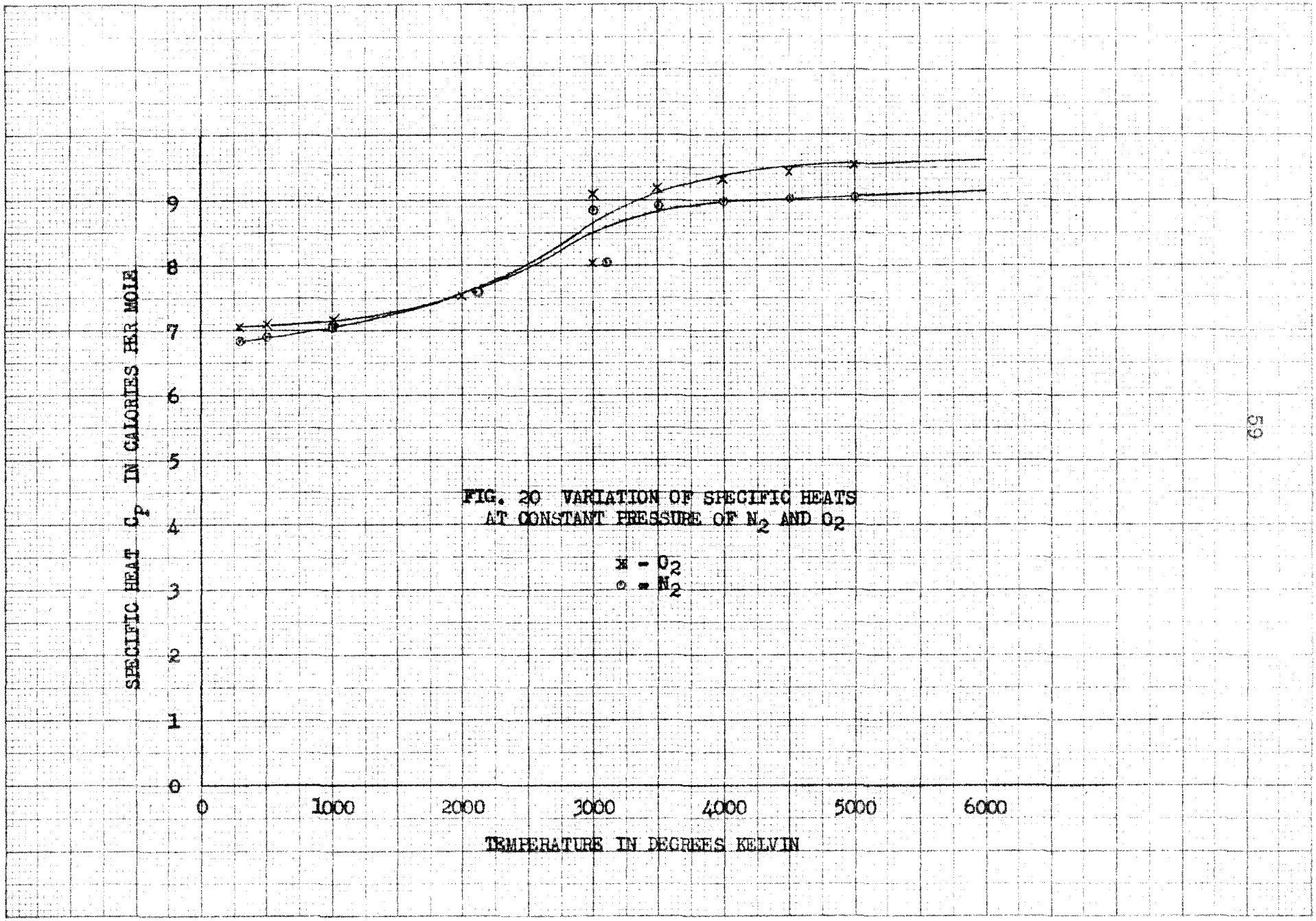

FIG. 20 VARIATION OF SPECIFIC HEATS AT CONSTANT PRESSURE OF N_2 AND O_2

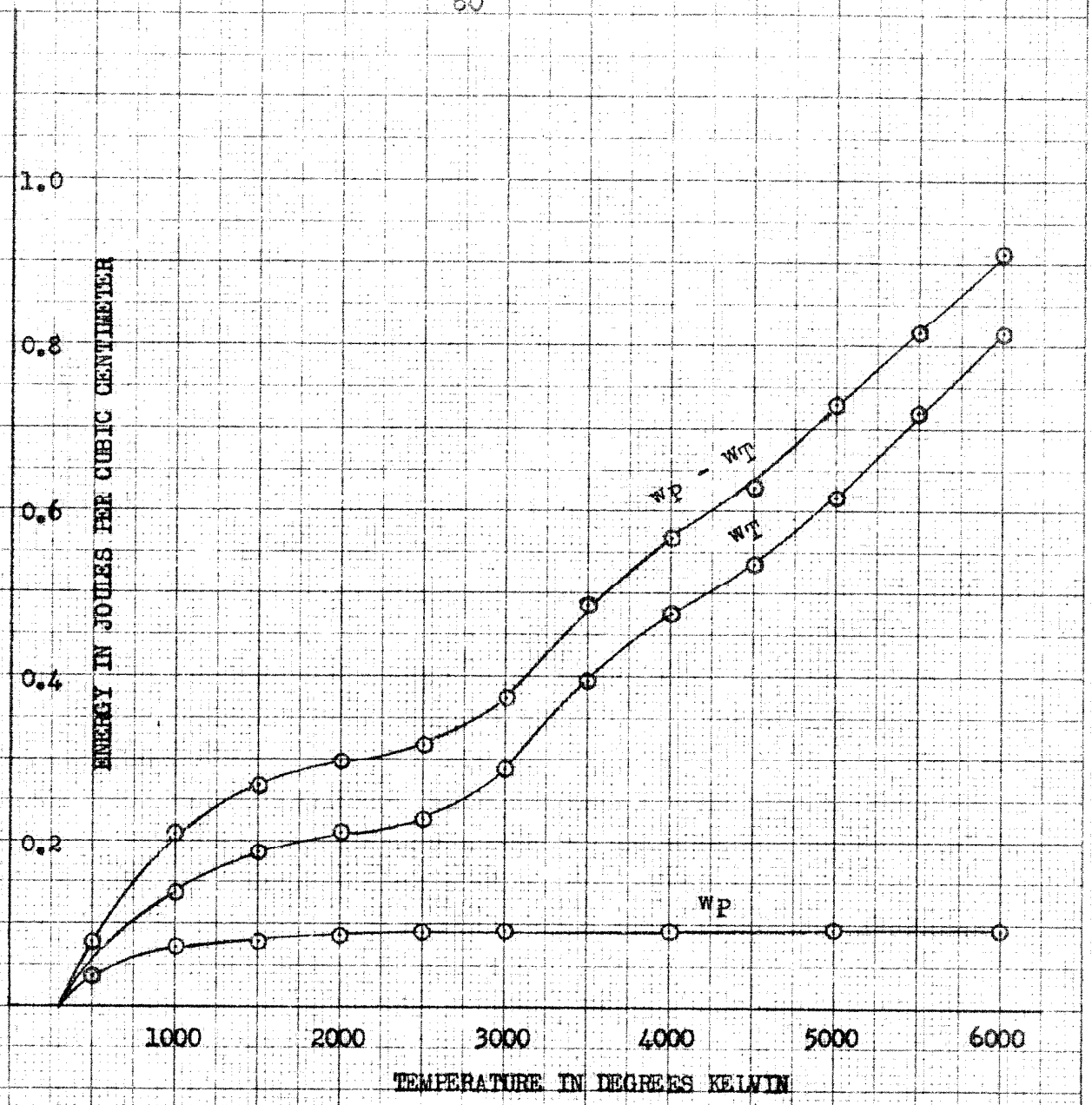

FIG. 21 ENERGY CONTENT OF AIR PER CUBIC CENTIMETER ABOVE THAT CONTAINED AT 300 DEGREES KELVIN

Appendix B

Discussion of the Variation of the First Townsend Ionizing Coefficient with Temperature

For convenience, consider a pure gas which is diatomic at normal temperature and appreciably dissociated at high temperature, say 3000° K. A good expression for the first ionizing coefficient of the pure diatomic gas is given below. The formula is due to v. Engel and Steenbeck (See Loeb (16) pg. 368) and can be written in the following form for constant pressure

$$\alpha = \frac{2.42\times10^{6} V_i a(Ta/T)}{\sqrt{f}} \epsilon^{\frac{-2.11\sqrt{f}\,V_i}{X\lambda_a(T/Ta)}} \left\{1 + \frac{2.11\sqrt{f}\,V_i}{2X\lambda a(T/Ta)}\right\}$$

Here, V_i is the ionization potential of the gas, T is the gas temperature with value T_a at normal temperature, λ_a is the electron mean free path at temperature T_a, X is the field strength, f is the fractional loss of electron energy on collision, a is a constant of the gas, and α is the ionizing coefficient in ionizations per unit length.

As long as the gas is purely diatomic, all quantities in the above equation are constant except the mean free path $\lambda a(T/Ta)$. This is a variation of α with gas density and has already been accounted for by the use of Fig. 16. When the gas is appreciably dissociated, the mean free path is no longer given by $\lambda a(T/Ta)$; however, since X appears in the exponent, it is difficult to see how this could account for a change in X at sparking of more than a factor of two. This follows since the Townsend sparking criterion (See Loeb

(16) pg. 409) is so very much more dependent on α than the second coefficient γ.

The value f should change with changes in the molecular nature of the gas. The value of f should be different for the diatomic gas than for the dissociated gas. This is true because of the larger number of excitations made possible by the rotational and vibrational states. As mentioned before, since X appears in the exponent, small variations in f can be compensated by even smaller changes in X.

Although the variations mentioned above do exist, it is doubtful that they could account for the actual range of variation of the recovery dielectric strength after the change with density has been considered. Also, sparking discharges are not of the 'long-tail' variety shown in Fig. 18. Evidently, the recovery dielectric strength and its variation depend on the gas density and the residual ion density.

Appendix C

The Diffusion of Ions in the Arc Space During Recovery

The diffusion of a gas or of ions in a field free region is governed by the diffusion equation

$$D \nabla^2 n = \frac{\partial n}{\partial t} \tag{1}$$

where n is the density and D is the diffusion coefficient (16). For the case of ion diffusion, the region can not be field free unless the density of positive and negative ions are the same. If this is the case and, say, the negative carriers have the greater diffusion coefficient, their motion will be retarded by space charge fields; i.e. the faster negative ions will aid the diffusion of the heavier positive ions while the negative ion diffusion will be retarded. The diffusion of the ions is then dependent on the ambipolar diffusion coefficient

$$D = (D_+K_- + D_-K_+)/(K_+ + K_-) \tag{2}$$

Consider the following simplified picture as applying in the case of diffusion from the arc core during the recovery period. In cylindrical coordinates, the ion density is a function of the radius and time only. At time $t = 0$, the density is constant $n = n_o$ for $r < r_o$ and $n = 0$ for $r > r_o$.

Then,

$$\frac{1}{r} \frac{\partial}{\partial r} \left(r \frac{\partial n}{\partial r}\right) = \frac{1}{D} \frac{\partial n}{\partial t} \tag{3}$$

If Eq. 3 is solved by taking

$$n = R(r)\,T(t)$$

in Eq. 3 and separating variables, there results

$$(4) \qquad \frac{\frac{1}{r}\frac{dR(r)}{dr} + \frac{d^2R(r)}{dr^2}}{R(r)} = \frac{1}{D}\frac{dT(t)}{T(t)} = -y^2$$

where y is an undetermined constant. From Eq. 4, it is observed that a general solution of Eq. 3 is

$$(5) \qquad n = \int_o^\infty yf(y)\,\epsilon^{-Dy^2t} J_o(ry)\,dy$$

Since Eq. 5 must hold for all t, the boundary conditions at t = 0 and the Fourier-Bessel integral allow the determination of f(y). The Fourier-Bessel integral states

$$(6) \qquad f(u) = \int_o^\infty vJ_n(vu)\left[\int_o^\infty yf(y)J_n(vy)\,dy\right] dv$$

On substitution of the boundary conditions and Eq. 5 in Eq. 6, there results

$$f(u) = \int_o^{r_o} vJ_o(vu)n_o\,dv$$

or

$$(7) \qquad f(u) = \frac{n_o}{u^2}\, r_o u\, J_1(r_o u)$$

Eq. 7 in Eq. 5 gives the required solution

$$(8) \qquad \frac{n}{n_o} = \int_o^\infty J_1(r_o y)J_o(ry)\,\epsilon^{-Dy^2t}\,d(r_o y)$$

The ion concentration is greatest on the axis r = 0 where

$$(9) \qquad \frac{n}{n_o} = \int_o^\infty J_1(r_o y)\, \epsilon^{-Dy^2 t}\, d(r_o y)$$

Watson (21) gives the definite integral

$$(10) \qquad \int_o^\infty \epsilon^{-p^2 t} J_1(\alpha t)\, dt = \frac{\sqrt{\pi}}{2p}\, \epsilon^{-\frac{\alpha^2}{8p^2}}\, I_{1/2}\left(\frac{\alpha^2}{8p^2}\right)$$

While Smythe (22) shows

$$(11) \qquad I_{1/2}(\partial) = \sqrt{\frac{2}{\pi\partial}}\, \sinh \partial$$

If Eq. 10 and Eq. 11 are used to evaluate the integral of Eq. 9, there results

$$(12) \qquad \frac{n}{n_o} = 1 - \epsilon^{-\left(\frac{r_o^2}{8Dt}\right)}$$

In order to substitute numbers in Eq. 12, consider Eq. 2 and

$$\frac{K+}{D+} = \frac{Ne}{P} = \frac{K-}{D-} \qquad \text{(see Loeb, pg. 170)}$$

Then

$$D = \frac{2K-D+}{K_+ + K-}$$

and since $K_- \gg K_+$, $D = 2\, D_+$. Now

$$D_+ = \frac{0.815\ C}{3}$$

where λ is the mean free path and C is the rms velocity. At 4800°K., D = 12 cgs. With an original current of 800

amperes crest and a current density of approximately 10 amperes per square centimeter, $r_o^2 \doteq 25$ so

$$(13) \qquad n/n_o \doteq 1 - \epsilon^{-250/t}$$

if t is expressed in milliseconds. On the basis of Eq. 13 it may be concluded that the diffusion is negligible during the recovery of the large open power arc in air.

Without restriction to a particular coordinate system, consider the expression for the mean square of the distance of the particles from the origin

$$\overline{Nr^2} = \int_v nr^2 d\tau$$

If Eq. 1 is substituted in this equation, the resulting equation may be integrated with the aid of the Green's Theorem whence

$$\frac{d}{dt} \overline{r^2} = 6D$$

Upon substitution of numbers, the same conclusion as above results.

Bibliography

1. J. Slepian, Extinction of an A-C Arc, A.I.E.E. Transactions, Vol. 47, 1928, pg. 1398
2. J. Slepian, Extinction of a Long A-C Arc, A.I.E.E. Transactions, Vol. 49, 1930, pg. 421
3. Philip Sporn and D. C. Prince, Ultrahigh-Speed Reclosing of High-Voltage Transmission Lines, A.I.E.E. Transactions, Vol. 56, 1937, pg. 81-90
4. Philip Sporn and C. A. Muller, Experience with Ultrahigh-Speed Reclosing of High-Voltage Transmission Lines, A.I.E.E. Transactions, Vol. 58, 1939, pg. 625-631
5. A. C. Boisseau, B. W. Wyman, and W. F. Skeats, Insulator Flashover Deionization Times as a Factor in Applying High-Speed Reclosing Circuit Breakers, A.I.E.E. Transactions, Vol. 68, 1949
6. G. D. McCann, J. E. Conner, and H. M. Ellis, Dielectric-Recovery Characteristics of Power Arcs in Large Air Gaps, A.I.E.E. Transactions, Vol. 69, 1950
7. H. M. Ellis, Factors Affecting the Rate of Dielectric Recovery of Power Arcs in Long Air Gaps, PhD, Thesis, California Institute of Technology, 1950
8. L. S. Ornstein, Physica 1, 1934, pg. 797
9. R. Mannkopf, Z. Physik, 86, pg. 161
10. C. G. Suits, Physics, Vol. 6, pg. 190, pg. 315, 1935

11. Leon Blitzer and W. M. Cady, Excitation Temperature in Time-Resolved Spectra of Single Condensed Spark Discharges, Journal Optical Society of America, Vol. 41, 1951, pg. 440

12. K. B. King and A. S. King, Relative f-Values for Lines of FeI and TiI, Astrophysical Journal, Vol. 87, 1938, pg. 24

13. W. W. Carter, Measurement of f-Values in the Iron Spectrum with Applications to Solar and Stellar Atmospheres, Physical Review, Vol. 76, 1949, pg. 962

14. H. Hemmendinger, Electrode Concentrations and Total Intensity of Spectral Lines, Journal Optical Society of America, Vol. 31, 1941, pg. 150

15. H. N. Russell and Charlotte E. Moore, The Arc Spectrum of Iron (Fe I), Part I, Transactions of the American Philosophical Society, New Series-Vol. 34, Part II, 1944, pg. 113-179

16. L. B. Loeb, Fundamental Processes of Electrical Discharge in Gases, Book, John Wiley and Sons, 1939

17. C. Kenty, Physical Review, Vol. 32, 1928, pg. 624

18. F. L. Mohler, Bureau of Standards Journal Research; Vol. 10, 1931, pg. 771; Vol. 19, 1937, pg. 447; Vol. 19, 1937, pg. 447

19. R. A. Johnson, B. T. McClure, R. B. Holt, Electron Removal in Helium Afterglows, Physical Review, Vol. 80, 1950, pg. 376

20. C. G. Suits and Hillel Poritzky, Physics, Vol. 6, 1935

21. G. N. Watson, Theory of Bessel Functions, Book, Cambridge, 1922, pg. 394

22. W. R. Smythe, Static and Dynamic Electricity, Book, McGraw-Hill, 1950, pg. 197